

UNIVERSITY OF BIRMINGHAM



The effect of microstructure and composition on HDDR processing of scrap magnets.

by

Alec James Durrant

A thesis submitted to the University of Birmingham for the degree of Master of Research

Metallurgy and Materials
University of Birmingham
Edgbaston
Birmingham
B15 2TT

April 2013

UNIVERSITY OF
BIRMINGHAM

University of Birmingham Research Archive

e-theses repository

This unpublished thesis/dissertation is copyright of the author and/or third parties. The intellectual property rights of the author or third parties in respect of this work are as defined by The Copyright Designs and Patents Act 1988 or as modified by any successor legislation.

Any use made of information contained in this thesis/dissertation must be in accordance with that legislation and must be properly acknowledged. Further distribution or reproduction in any format is prohibited without the permission of the copyright holder.

Abstract

Due to increasing pressure on the supply of rare earth metals there is a growing need to develop recycling strategies for rare earth containing materials. The aim of this investigation was to use the Hydrogenation Disproportionation Desorption Recombination (HDDR) processing technique to recycle sintered magnets and cast rare earth alloys based upon neodymium iron boron (NdFeB). The study investigated the impact of microstructure and composition on the HDDR processing conditions and resultant magnetic properties of the NdFeB powders. Heat treatment techniques were used to alter the grain size of sintered magnets to simulate a variety of NdFeB feedstock for HDDR recycling. To investigate the effect of the composition on HDDR recycling process a comparison between two cast alloys with varying Nd content was undertaken. The HDDR powder created by the recycling process was assessed using a vibrating sample magnetometer (VSM). Microstructural analysis was carried out using optical and backscattered scanning electron microscopy.

This study demonstrated that it is possible to develop significant anisotropy using the HDDR process on sintered NdFeB-type magnets. However the same processing conditions could not be applied to materials with larger grain sizes or cast materials. This study also explains the effect heat treatments can have on the development of soft magnetic phases.

Acknowledgements

I would like to give my thanks to the University of Birmingham for the opportunity to carry out this research project. In particular I would like to send thanks and dedicate this thesis to the late Andy Williams, without whom this project would not have been possible. Furthermore I would like to give thanks for the work and help of Allan Walton, whose advice was invaluable. I would also like to thank the entire Hydrogen and Magnets department including Richard Sheridan, Mal Degri and Jonathan Meakin for their contributions.

Finally a big thank you goes to my family and girlfriend who have supported and encouraged me throughout the course of the project.

Contents

Abstract.....	2
Acknowledgements	3
Contents	4
Introduction	1
1.1 Rare Earth Magnet Market	1
1.2 History Of Magnets	3
1.3 Current Applications of Rare Earth Magnets.....	6
2.....	9
Literature Review	9
2.1 Magnetic Materials	9
2.1.1 Magnetic Quantities.....	9
2.1.3 Categories of Magnetism	11
2.1.4 Domains.....	14
2.1.5 Single Domain Particles.....	16
2.1.6 Permanent Magnets.....	17
2.1.7 Hysteresis Loop	17
2.1.8 Magnetocrystalline Anisotropy.....	19
2.1.9 Coercivity Mechanisms	21
2.2 NdFeB Magnets	24
2.2.1 Importance of Fe and Nd	24
2.2.2 The Magnetic Phase – $Nd_2Fe_{14}B$	26
2.2.3 The Nd-Rich Phase	27
2.2.4 The $NdFe_4B_4$ Phase.....	28
2.2.4 The Nd_2Fe_{17} Phase	28
2.3 Manufacturing Processes for NdFeB Magnets	28
2.3.1 Sintered NdFeB.....	29
2.3.2 Resin Bonded NdFeB Magnets	32
2.4 The Effect of Additives on HDDR Processing	42
2.4.1 Cobalt	42
2.4.2 Dysprosium	43
2.4.3 Aluminium.....	44
2.4.4 Copper	45
2.4.5 Niobium	46
2.5 The Effect of Oxygen Content on HDDR Processing.....	47

2.6 Hydrogen Recycling Techniques for NdFeB Magnets	48
2.6.1 Separation and Extraction Techniques.....	49
2.6.2 Reprocessing Routes.....	50
2.6.3 Recycling using the HDDR process.....	51
3	55
Experimental Procedure.....	55
3.1 Starting Materials.....	55
3.2 Heat Treatment	55
3.3 Hydrogen Decrepitation.....	56
3.4 HDDR.....	56
3.5 Testing Magnetic Properties	57
3.6 Microstructure Analysis.....	58
4.....	59
Results and Discussion	59
4.1 The effect of microstructure on HDDR processing	59
4.1.1 Microstructural analysis of starting materials	60
4.1.2 Altering Microstructure- Disproportionation curves.....	67
4.1.3 Microstructural analysis of HDDR material	70
4.1.4 Altering Microstructure- VSM Traces	73
4.2 Comparing sintered magnets with the different compositions	76
4.2.1 Comparison between Sintered Magnets- Disproportionation Curves	77
4.2.2 Comparison between Sintered Magnets – VSM results.....	79
4.3. An investigation into HDDR processing of cast materials with varying Nd content.....	81
4.3.1 Altering Nd Content- Disproportionation curves.....	82
4.3.2 Altering Nd content- VSM results.	85
5	88
Conclusion	88
5.1 The effect of microstructure on HDDR processing	88
5.2 Comparison between sintered magnets with different compositions.....	88
5.3 Altering Nd content in cast alloys.....	89
5.4 Summary.....	90
6	91
Future Work.....	91
References	92
Appendix	97

Introduction

1.1 Rare Earth Magnet Market

Rare earth magnets are vital components in a wide range of devices including DVD and CD players, hard disc drive motors, MRI scanners, motors in automobiles and generators in wind turbines. The global market demand for these materials has rapidly increased since their introduction in the late 1980s. There are two types of rare earth magnet, which are either based on samarium cobalt alloys (SmCo_5 or $\text{Sm}_2\text{Fe}_x\text{Cu}_x\text{Zr}_x\text{Co}_{17}$) or neodymium iron boron (NdFeB). This project focuses on is the NdFeB-type magnets. NdFeB magnets contain the rare earth element neodymium (Nd), with lesser amounts of dysprosium (Dy) and niobium (Nb). NdFeB-type magnets are the most powerful permanent magnet known to man.

Despite being known as rare earth metals these elements are fairly abundant in the earth's crust. However they are difficult and expensive to extract from the ore, as it contains many rare earth metals, which are mixed together. The mixtures of rare earths are chemically very similar and readily form stable oxides. The rare earth ores often also contain radioactive material such as thorium, making extraction hazardous. The extraction processes are also very polluting, as the chemicals and leachants used to extract the rare earths from their ores, are often poured into excavated craters forming 'tailing' lakes.

China currently produces 97% of the world's rare earths metals, including Nd and Dy, despite the fact that they only have 30% of the estimated world's reserves¹. China introduced export quotas and taxes in 2005 and in 2010 China cut its export quota by 40%.². As global demand has risen significantly in recent years (shown by the global rare earth consumption

(figure 2) this reduction in available rare earth supply had a significant impact on global market prices. From 2009-2011 the price of Nd rose from \$20/kg to around \$450/kg, with the price falling back down to around \$100/kg today. This increase in the price of Nd has further spurred new interest and research into the different possibilities for recycling of rare earth permanent magnets.

There are alternative ways to increase the supply rare earth metals, for example by re-opening mines elsewhere in the world. Many mines were forced to close when China flushed the market with cheap rare earth material in the 1990's. However with increased demand and higher market costs mines are now re-opening in the U.S.A (Mountain Pass), South Africa (Steekampsraal) and Australia (Mount Weld). An alternative option would be to use devices which do not contain rare earth metals. An example would be the use of induction technology in place of permanent magnet generators in wind turbines. However this would lead to a drop off in efficiency of the device and result in an increased maintenance costs³.

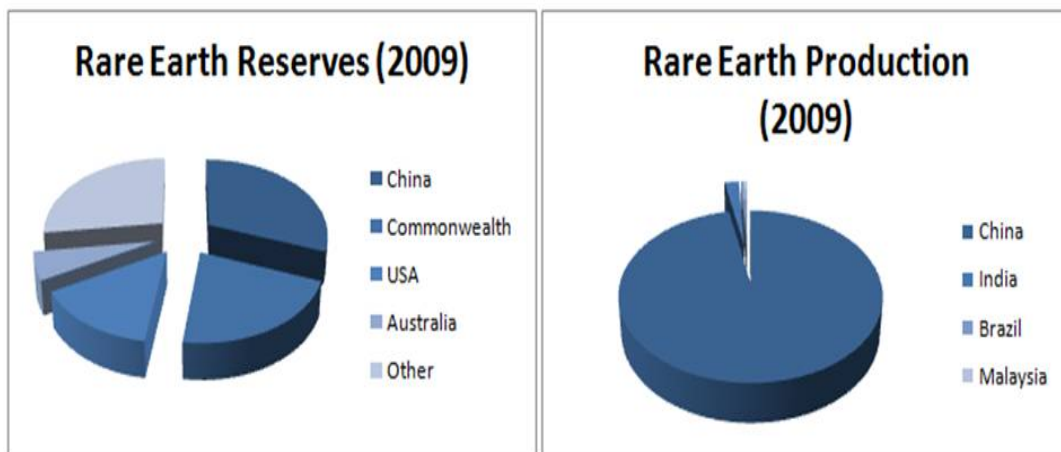


Figure 1. Global Reserves of Rare Earth compared to Global Production¹

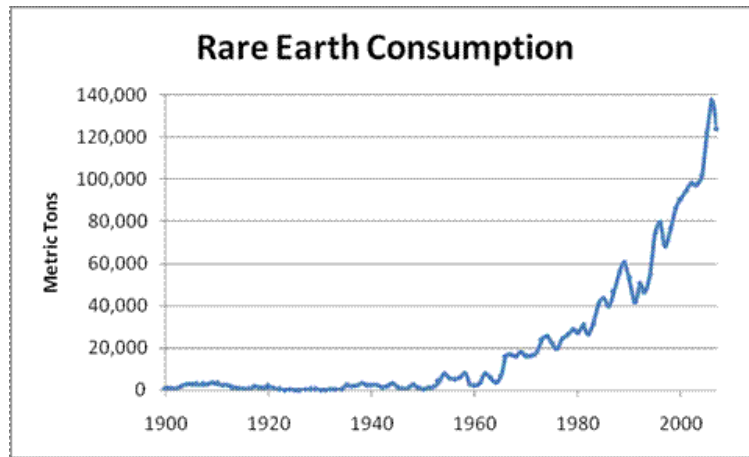


Figure 2. *Global Rare Earth Consumption over the 20th century*¹

The large number of benefits of rare earth magnets over existing alternatives is expected to continue to drive demand for these materials for many years into the future⁴.

1.2 History Of Magnets

The history of magnets can be traced back over many centuries. The Chinese were one of the first cultures to present references in the literature of a material which had the ability to “summon iron”. Lodestone (Fe_3O_4) is a naturally occurring oxide and was the first magnetic materials to be recognised. This gave rise to the first application of a magnetic material, the compass. In 1600 the first studies were undertaken to understand magnetism by Dr William Gilbert who identified the Earth as being a large magnet. Until the 1800s investigations into magnetism and electricity were hypothetical. The link between electricity and magnetism was made unintentionally in 1820. Dr Hans Oerstead passed an electrical current through a wire and noted its effect on a nearby compass needle. This finding was later validated when the first electromagnets were conceived, which demonstrated that these materials were capable of supporting their own weight.

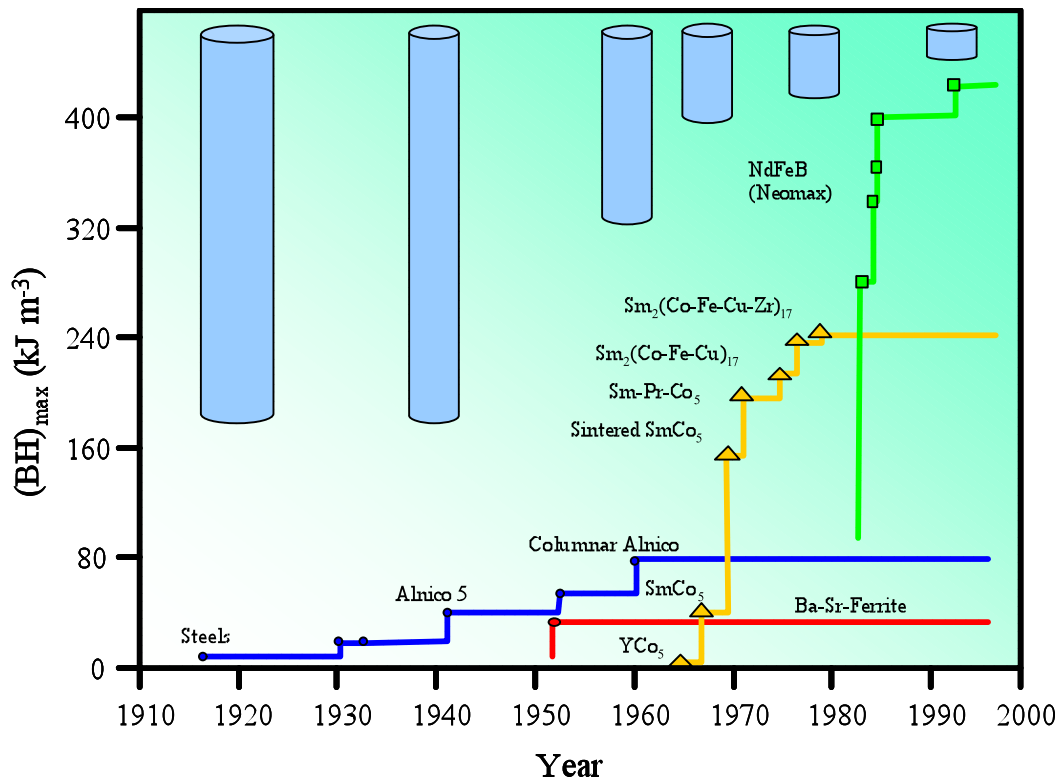


Figure 3: Permanent magnet development throughout the 20th century, showing the improvement of BH_{\max} and reduction in size over time.

There have been huge improvements in the performance of permanent magnets over the last century as shown in figure 3. The maximum energy product BH_{\max} is typically used as measurement of the performance of a permanent magnet. This is defined as the maximum field strength of a fully saturated magnetic material.

The first manufactured permanent magnet came of age in the 1930s, with the production of Co steel. This new material was important to the development of ‘Alnicos’ (alloys of Al, Ni, Co and Fe). Alnicos obtained their permanent magnetic properties through shape anisotropy, which arose due to the aspect ratio of non-spherical grains in the material (see Coercivity Mechanisms). Alnicos are still used in some applications today, due to their high Curie temperature $\sim 850^{\circ}\text{C}$.

In the 1950s ferrite magnets were discovered which are comprised of iron-rich mixed oxides, such as $\text{BaFe}_{12}\text{O}_{19}$ or $\text{SrFe}_{12}\text{O}_{19}$. These magnets demonstrated magneto crystalline anisotropy, leading to a relatively high coercivity. However as ferrites are ferrimagnetic materials, they have a low remanence and therefore a relatively low maximum energy product. Ferrite magnets are comprised of cheap materials and they are easy to manufacture. Ferrites also have excellent corrosion resistance.

The first rare earth magnets were developed in the 1960s based upon SmCo alloys. There are two different types SmCo_5 and $\text{Sm}_2(\text{Co}, \text{Fe}, \text{Cu}, \text{Zr})_{17}$ alloys both of which possessed very good magnetic properties. SmCo magnets resist thermal degradation, due to their high curie temperatures (720°C and 820°C respectively) and have good corrosion resistance. In the 1970s the price of Co increased rapidly due to problems with supply from Congo. This led to a push for other viable rare earth magnets, which did not include Co. Research focused on Nd-Fe alloys. Nd was selected as it was one of the most abundant of the light rare earths and it also has one of the largest 4f electron moments. Fe is by far the most abundant and accessible ferromagnetic 3d element, with one of the largest 3d magnetic moments. However no high iron content binary Nd-Fe magnet exists.

In 1982 two independent companies announced, simultaneously, the discovery of an NdFeB-type magnet. Sumitomo Special Metals in Japan developed a powder metallurgy processing routes for $\text{Nd}_{15}\text{Fe}_{77}\text{B}_8$ permanent magnets with an energy product of 290kJ/m^3 . In the USA General Motors led a parallel line of research into the production of melt spun NdFeB-type magnets. Both groups realised that the principle magnetic phase was a tetragonal compound identified as $\text{Nd}_2\text{Fe}_{14}\text{B}$. NdFeB-type magnets have a high saturation magnetisation but the Curie temperature is only around 310°C .

1.3 Current Applications of Rare Earth Magnets

NdFeB-type magnets are used in a wide range of applications. To meet the growing demand for clean energy transport, the automotive industry has invested heavily into the use of permanent magnet motors to power hybrid and electric vehicles. An advantage of using a permanent magnet motor is their high efficiency. This is due to the motors simple design, with few moving parts and lightweight construction.

The Toyota Prius is one of the most common hybrid cars to date and has sold approximately 2,012,000 units around the globe since its release in Japan in 1997⁵. Each Prius has an AC Synchronous Permanent Magnet Brushless Direct Current (PMDC) motor that generates 60kW of power. Each Toyota Prius contains ~1-2kg of NdFeB magnet. Permanent magnets are also used elsewhere in cars; Brose a German automobile engineering company has been developing a range of brushless magnetic motors and generators. These find use in regenerative braking technology, electric window motors, drive systems for electric steering and cooling fan motors for ventilation⁶. These motors are said to be more reliable, efficient and smaller, compared to induction motors. These motors can lead to a CO₂ saving of 10%⁷.

The UK has by far the largest wind resource of any country in Europe and it has planned to install 33GW of offshore wind turbines by 2020. By using permanent magnets it is possible to design the wind turbine generator as a direct drive machine without a gearbox. This significantly reduces the maintenance costs of the device. Each direct drive wind turbine requires approx. 0.5tonnes of NdFeB-type magnet per MW⁸.

Another notable use of rare earth magnets is in electric bicycles. Each electric bicycle contains around 300-350g of NdFeB. In China alone there are approximately 100million electric bikes and this number is growing every year.

One of the largest uses of NdFeB type magnets today is in computer hard disc drives (HDD) motors, accounting for approximately 10-15% of the sintered NdFeB market. There are two magnets in a HDD. A sintered magnet in the voicecoil motor (VCM) assembly and a resin bonded magnet in the spindle motor, which spins the disk. Each HDD contains anywhere between 2-20grams of NdFeB magnet. At present most HDDs are shredded, to protect the data stored on the disc. NdFeB magnets are brittle and will break into a magnetic powder when shredded. This magnetic powder then sticks to any ferromagnetic components and is lost in the process.

Currently most of the redundant stock of scrap NdFeB magnets are in electrical equipment, such as HDDs. Magnets contained in electric vehicles and wind turbines will be in service for 10-15 years and 20-25 years respectively, so will not be available as scrap for some time. In order to recycle rare earth magnets, from electronics then an efficient extraction process is required. After separation of the magnet from the electronics then re-processing techniques are used in order to form a new magnet. Manual disassembly of the component and retrieving the magnet is one option; however this is time consuming and would require very cheap labour.

Hitachi Plant Technologies Ltd, disclosed the use of mechanical and chemical methods to separate rare earth elements from HDDs. The chemical processes left acidic and chemical waste, which required disposal. Recently Hitachi announced a new 'dry process' to extract rare earths using a special extraction medium with a high affinity for rare earths. This process is stated to reduce cost and the environmental burden of extraction.⁹ Hitachi aims to have this process running by 2013.

Workers at the University of Birmingham have disclosed a technology which uses hydrogen to reduce sintered NdFeB magnets into a demagnetised hydrided powder which can be

extracted using mechanical force¹⁰ (see chapter 2 for more details). It may be possible to then extract the rare earth elements from the hydrided powder in a similar fashion to Hitachi. It has also been shown that it is possible to re-process the extracted NdFeB hydrided powder directly from the alloy by re-sintering the material into new magnets. Alternatively the extracted powder can be reprocessed using the Hydrogenation Disproportionation Desorption Recombination (HDDR) route. The HDDR route modifies the microstructure of the material, making it suitable to form resin bonded magnets.

The aim of this research project is to optimise the HDDR processing route for a range of scrap feeds with varying composition, oxygen content and grain sizes i.e.

- Investigate microstructural effects of the starting material on HDDR processing.
- Investigate the effect of compositional variations on HDDR processing.

Literature Review

2.1 Magnetic Materials

2.1.1 Magnetic Quantities

A magnetic field H can be generated by passing an electric current Id through a coil of conductor with N turns. The magnitude of the magnetic field generated is given by:

$$H = NI$$

The current I is measured in amps and N is the number of coils per metre; therefore the magnetic field strength H is measured in Am^{-1} . This simple analysis assumes that H is solely determined by the magnitude and distribution of the current producing it, thus ignoring the effect of any material present.

When a magnetic field H is applied to a material the reaction it undergoes is known as its magnetic induction B . Magnetic induction is a measure of the total flux through a unit of cross sectional area. Every material will respond with some degree of induction to an applied magnetic field, the relationship between the response of the material and the applied magnetic field is called the permeability μ . The permeability of is given by:

$$\mu = B/H$$

A property closely related to the permeability is the susceptibility χ . This is simply the ratio of magnetisation M and the field H and is expressed as:

$$\chi = M/H$$

Here the magnetisation is measured as the magnetic moment per unit volume of a solid in (Am^{-1}). The susceptibility gives the characteristics of the magnetic material by measuring how a given material reacts to the application of a field. The relative permeability μ_r of a free space is 1 a constant; the relative permeability has a close relationship also with susceptibility and is expressed as:

$$\mu_r = \chi + 1$$

The μ_r of a material is given by:

Where μ_0 is the permeability of free space with a value of $4\pi \times 10^{-7}$ and is measured in (volts per second)(amp meter) known as Henries per meter (Hm^{-1})

Magnetic induction B is a result of the combination of two factors; firstly M and second is H . The contribution of the applied magnetic field and the magnetisation are termed $\mu_0 H$ and $\mu_0 M$ respectively. Therefore magnetic induction can be seen to be a vector sum of the two.

$$B = \mu_0 (H + M)$$

This equation will measure the magnetic properties of the entire system, including the applied current. In order to measure the properties of the material itself it is important to consider the intrinsic quantity of the magnet J , which is expressed as:

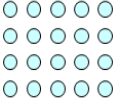
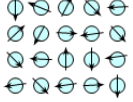
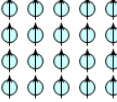
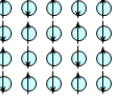
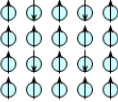
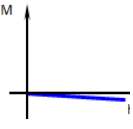

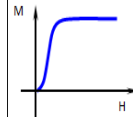
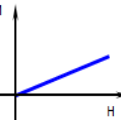
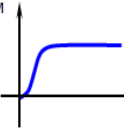
$$J = \mu_0 M$$

Unlike B , which will increase indefinitely with increase of applied field, the alignment or polarisation of a material will reach a maximum value, known as the saturation point or J_s .

2.1.3 Categories of Magnetism

Every material known to man can be categorised by its magnetic properties and will fall into one of the five categories of magnetism as shown in table 1.

Table 1: Categories of Magnetism

Type of Magnetism	<i>Dia-magnetism</i>	<i>Para-magnetism</i>	<i>Ferro-magnetism</i>	<i>Antiferro-magnetism</i>	<i>Ferri-magnetism</i>
Magnetic Moment					
Example and Magnitude	Au -2.74x 10 ⁻⁶ Cu - 0.77x 10 ⁻⁶ Bi -16.6x 10 ⁻⁶	βSn 0.19x 10 ⁻⁶ Pt 21.04 x 10 ⁻⁶ Mn 66.1x 10 ⁻⁶	Fe 100,000	Cr 3.6x10 ⁻⁶	Ba Ferrite 3
Susceptibility					

2.1.3i Diamagnetism

Diamagnets are solids with no permanent magnetic moment per atom because of their filled electron shells. Diamagnetism results from a change in orbital motion of electrons when an external magnetic field is applied. The application of an external field will cause the electron orbitals to re-align in the direction of the applied field. This causes an opposing force resulting in a small and negative susceptibility, repelling the magnetic flux from the material. The repelling field typically has an order of magnitude of approximately 10^{-5} to 10^{-6} . Bismuth is one of the most well-known diamagnetic materials.

2.1.3ii Paramagnetism

Paramagnetic materials are composed of atoms with a permanent magnetic dipole moment i.e. non filled electron shells. However in the absence of an applied field these dipole moments are arranged in a random orientation and the material will exhibit no overall net magnetic moment. When an external field is applied, the orbital motion of the electrons is aligned and contributes to a small net magnetisation, but the susceptibility is very small.

2.1.3iii Ferromagnetism

Ferromagnetism is the strongest type of magnetism. In ferromagnetic materials the magnetic dipole moments are aligned without an external applied magnetic field, resulting in spontaneously magnetisation. However ferromagnetic materials can exist in a demagnetised state due to magnetic regions called domains (see section 2.1.4). When a field is applied all the magnetic domains within a material align and it reaches its saturation point. The value of the magnetic saturation of ferromagnetic materials depends strongly on temperature, decreasing from a maximum value slowly as it approaches its Curie temperature T_c . Once above this temperature the material will then act as a paramagnet. The Curie temperature can be derived using the following expression:

$$\chi = C/T$$

Where χ is the magnetic susceptibility of the ferromagnet, C is the material specific Curie constant and T is the absolute temperature measured in kelvin.

In order to understand the process which gives rise to ferromagnetism it is first important to understand the interactions which give rise to the parallel alignment of dipoles. Dr Werner Heisenberg was the first to show how the exchange interaction between electrons of neighbouring atoms in incomplete subshells could lead to parallel alignment. Dr John Slater later showed how the values of interatomic distances r_{ab} and the radii of incomplete filled electron sub shells r_d varied. It was observed that the values of r_{ab}/r_d correlated with Heisenberg's exchange interaction. Dr Hans Bethe then obtained the exchange integral as a function of interatomic spacing between the electrons and the respective nuclei resulting in the Bethe Slater curve (figure 4). Elements with a positive exchange integral can be classified as ferromagnetic and those with a negative value as antiferromagnetic.

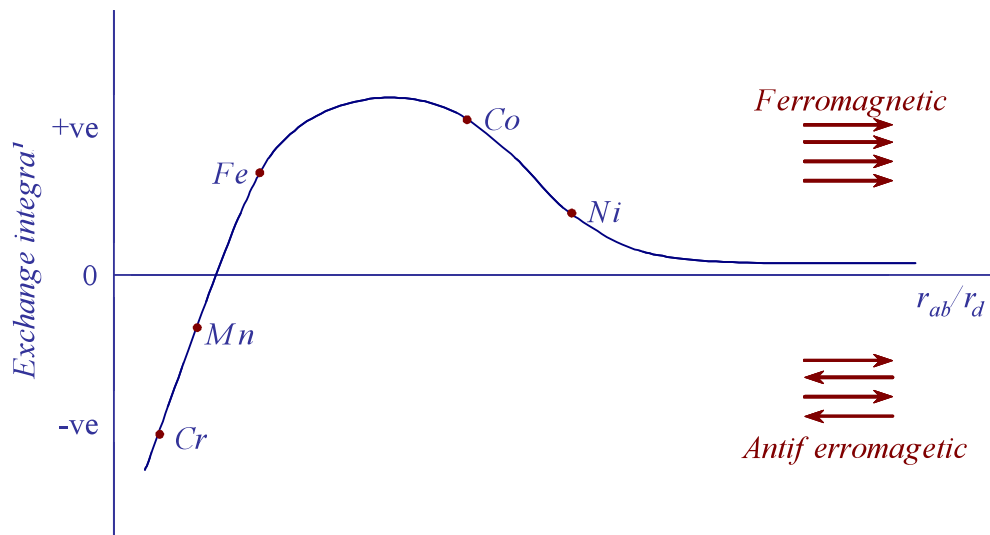


Figure 4: Bethe-Slater Curve

2.1.3iv Anti-Ferromagnetism

In antiferromagnetic materials, the magnetic dipoles are aligned in opposite directions i.e. anti-parallel. Under an applied field these materials act in a similar fashion to those of paramagnets, generating a small positive susceptibility of a similar magnitude.

2.1.3v Ferrimagnetism

Ferrimagnets are a material very similar to that of anti-ferromagnets, as each has anti-parallel magnetic dipoles. In ferrimagnetic materials the exchange interaction causes the magnetic moments of sub-lattices of atoms to align parallel or anti-parallel to each other. However different to anti-ferromagnets the magnetic moments are unequal resulting in a net magnetisation in that direction. Ferrite magnets are examples of ferrimagnetic materials.

2.1.4 Domains

To be able to explain how ferromagnetic material can exist in the demagnetised state, despite having spontaneous magnetisation. French physician Pierre-Ernest Weiss proposed the concept of magnetic domains in 1907. He suggested that within an area of magnetic material there were a large number of aligned magnetic moments $\sim 10^{12} - 10^{18}$, this area was described as a domain. Within domains the magnetisation is almost saturated, however the overall domain alignment is random throughout the material.

In order to cause the domains to align within the material and therefore magnetise the material an external field is applied (see figure 5). Initially this field will cause the domains which are aligned favourably with the applied field to grow in size, with a respective reduction in the number of domains which oppose the applied field. As a result the material develops a weak magnetisation in the direction of the applied field. The second mechanism which occurs as the applied field strength increases is domain rotation. Within the remaining unfavourably aligned atomic moments the applied field strength overcomes the anisotropy energy. This causes the domains to rotate from their original direction to align along the crystallographic easy axis in

the general direction of the applied field. A process known as coherent rotation is the final process to occur in domain alignment, as the field is further increased. The final magnetic moments, which are aligned close to that of the applied field, are gradually rotated from their easy axis, until they are parallel in orientation to the applied magnetic field.

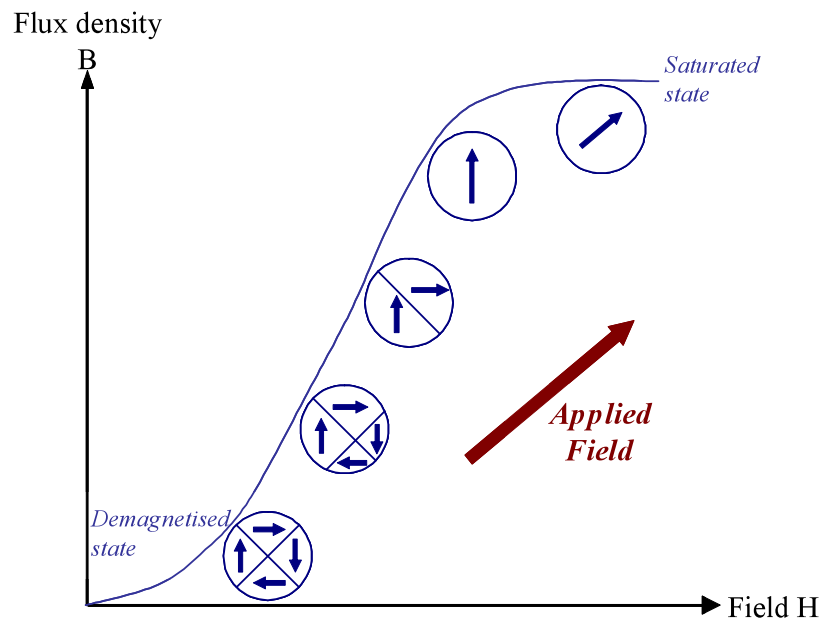


Figure 5: Magnetisation curve of a ferromagnetic sample, showing the influence of applied field on domain structure.

The reason for the existence of magnetic domains within a material is to reduce the total energy of the system. A uniformly magnetised single domain sample is shown in figure 6.a. which has a magnetostatic energy associated with it. This is due to the magnetic material containing free poles on the surface. At the top “north poles” and at the bottom “south poles” which between them generate a demagnetisation field H_d . Within the specimen the magnetisation will point from the south to the north, while the direction of the magnetic field generate will run from the north to the south pole. This is the same principle which applies for magnetic moments within a single dipole. In magnets the rise of this external flux field will oppose that of the internal magnetisation field, due to it being opposite in direction and

strength. It is also dependant on the geometry and degree of magnetisation of the sample. Thus the opposing H_d generated creates an unstable situation within the material.

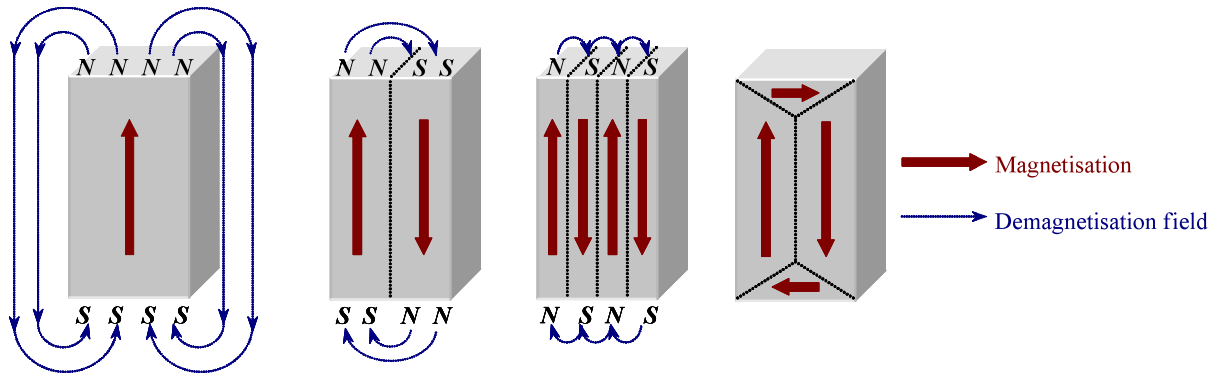


Figure 6: Illustration showing the division of magnetisation into domains a) single domain b) two-domains c) multi-domains d) closure domains.

By separating the magnetisation into two domains (figure 6.b.) this reduces the magnetostatic energy by half. By having both a north pole (left) and south pole (right) on the top surface, with the opposite being true on the bottom results in the demagnetisation field being confined to areas near the top and bottom of the specimen. This reduces the total area affected by the demagnetisation field, stabilising the material. Further subdivision (figure 6.c.) will reduce the magnetostatic energy more and further stabilise the specimen. Figure 6.d. shows a domain pattern known as a closure domain. These are usually found in materials with a cubic atomic structure such as iron i.e. materials which do not exhibit any uniaxial anisotropy (see section 2.1.8). These domains will form at the early stages of magnetisation as they provide a return path for the magnetic flux within the material. The specimen will continue to divide into further domains if the reduction in magnetic energy overcomes the energy required to form more domain walls.

2.1.5 Single Domain Particles

Grain boundaries are areas of high energy within polycrystalline materials. Increasing the volume fraction of grain boundaries, by reducing the total grain size, will lead to an increase

in strength of the material. This is attributed to the dislocation movement of the material being hindered by the grain boundaries. In magnetic materials the domains behave in a similar manner. The domain wall has an energy associated with it. If the grain/particle size is reduced in size then eventually the domain wall energy becomes greater than the magnetostatic energy, such that the grain can only contain a single domain.

The single domain nature of these types of materials will have an impact on the coercivity mechanisms exhibited by these magnets. (Shown in section 2.1.8iii)

2.1.6 Permanent Magnets

A permanent magnet will retain its magnetism when an external magnetic field is removed. All commercial permanent magnets contain ferrites. Once magnetised these materials attract other ferromagnetic materials towards them. However ferromagnets can be divided into two categories, ‘soft’ and ‘hard’. Soft ferromagnets, such as iron, can be magnetised but are also very easily demagnetised. Permanent magnets are known as hard ferromagnets are not easily demagnetised and have a typically high coercivity value (10kA/m) . NdFeB-type magnets are an example of ferromagnets. One of the easiest ways of representing the difference between ‘soft’ and ‘hard’ magnetic materials is to use a hysteresis loop.

2.1.7 Hysteresis Loop

A hysteresis loop is a measure of the magnetisation/polarisation or induction against an applied magnetic field and is normally plotted in four quadrants (figure 7). The curve shows a plot of the magnetic induction B under various applied fields H . It is possible to substitute magnetisation $\mu_0 M$ for B since:

$$B = \mu_0 (H + M)$$

Note. $\mu_0 M$ or J is also usually plotted as they share the same units (Tesla) and can therefore be plotted on the same axis as B .

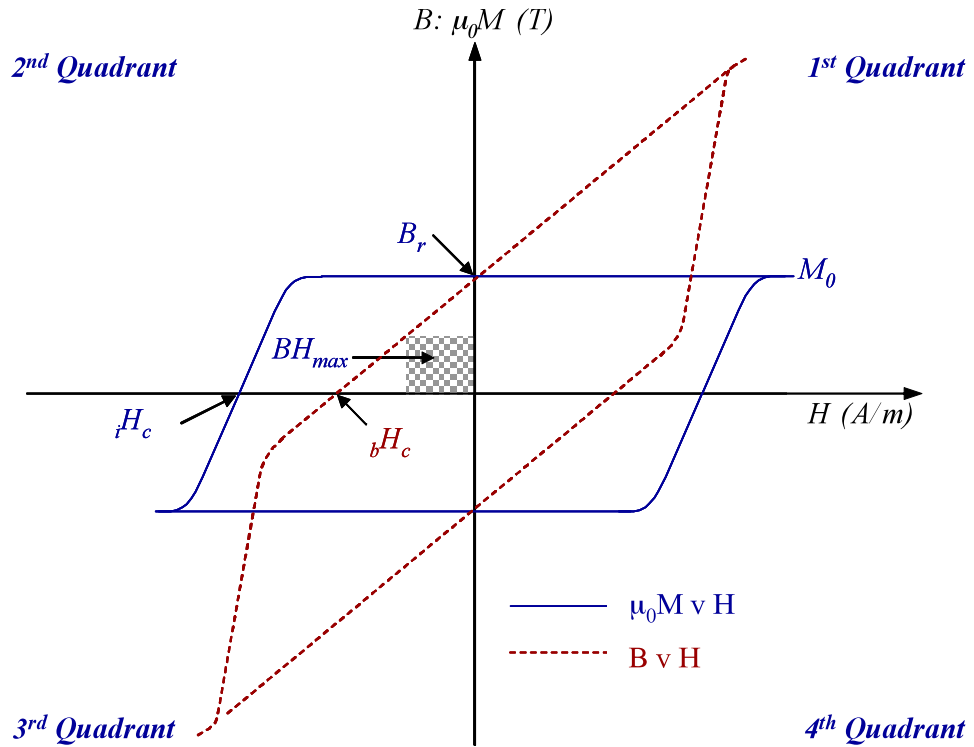


Figure 7: A magnetic hysteresis loop, showing magnetic induction and applied field curves.

The application of an applied field H to a non-magnetised magnet will initially cause a rapid increase in magnetisation. Saturation magnetisation M_0 is reached when the increase in applied field no longer results in an increase in observed magnetisation. When the applied field is removed (reduced to zero) the remaining magnetic induction or remanance, B_r can be observed. The remanence is a key property for magnetic materials as this denotes the strength of a permanent magnet.

Applying a field in the reverse direction with a strength of H_c will reduce the magnetic induction to zero. The strength of the field required to demagnetise the material is known as the coercivity field and has two loops which will intersect the horizontal axis. The inductive coercivity ${}_bH_c$ which lies on the B versus H curve, is the sum of the magnetisation and applied field reaching zero i.e. $B=0$. The second line is the intrinsic coercivity ${}_iH_c$ which is where the magnetisation is falls to zero i.e. $\mu_0 M=0$. Both of these values can be used to measure the materials resistance to a reverse applied field. In soft magnetic materials both these values are

similar and usually no distinction is made between them. In hard magnetic materials however there is an obvious difference, iH_c is always a bigger value than bH_c .

Another important measure of magnetic materials is the maximum energy product BH_{max} . This is the maximum value of the product of magnetic induction B and applied field H . It is represented by the area of the largest square that will fit under the B versus H curve in the second quadrant of the hysteresis. For permanent magnets this figure represents a means of describing the performance of the magnet i.e. the larger the value the smaller the magnet to provide a useful amount of work.

Finally the ‘squareness’ of the M versus H loop in the second quadrant is often taken into account. It is used to gauge the degree of alignment and distribution of grains within the material. Calculated by obtaining the ratios of H to iH_c , where H is the reverse field applied to reduce the magnetisation to 90% of its remanent value. The squareness has values between 0 and 1.

2.1.8 Magnetocrystalline Anisotropy

Anisotropy is said to be present when the properties of a material differ depending on the direction of testing. In the case of magnets it is the variation of magnetic flux when tested along different axis of the material. One of the causes for this is known as magnetocrystalline anisotropy.

This is the property by which a material prefers to be magnetised along one or more crystallographic directions. Magnetocrystalline anisotropy occurs due a coupling of the spin and orbital motion of each electron with the crystal lattice. If the field is applied in the same direction as the preferred direction of magnetisation of the crystal lattice there will be little resistance to this field. This direction is known as the “easy” axis of the material. When the field is applied away from this “easy” axis of the material the resistance increases, until it is

applied perpendicular to the easy axis. This direction is known as the “hard” direction of magnetisation. Having measured the applied field in the easy and hard directions it is possible to create a magnetisation curve, shown in figure 8.

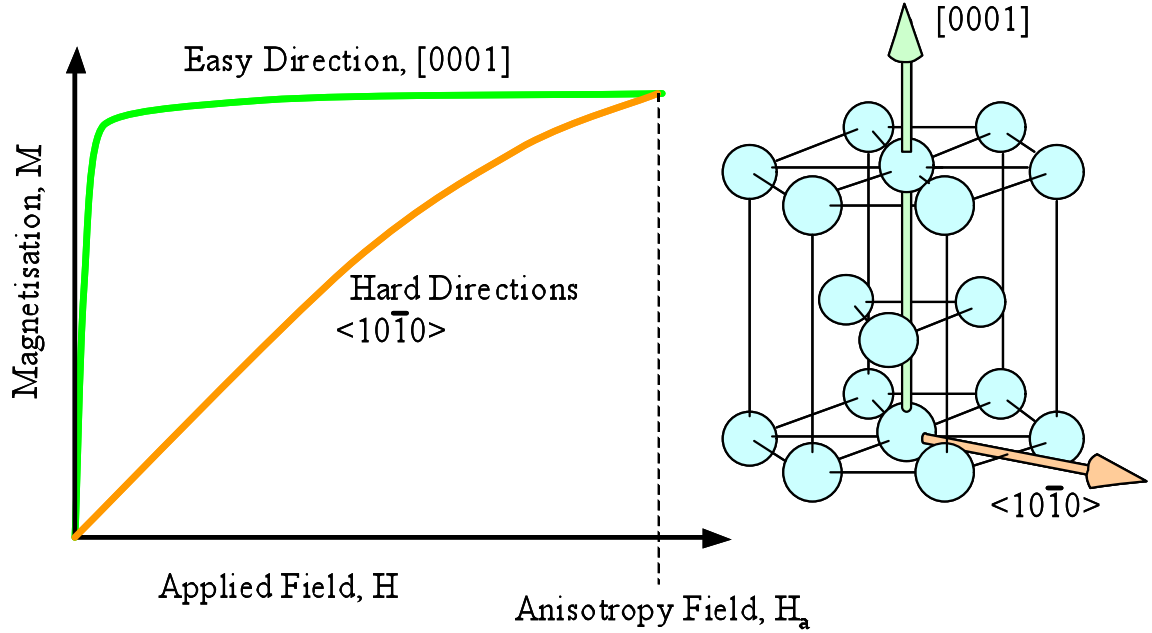


Figure 8: A magnetisation curve for a single crystal of Co. Showing measurements in the hard direction along the $[10\bar{1}0]$ axis and easy direction along the $[0001]$ axis.

The measure of magnetic “hardness” of the material in a specific orientation is known as the anisotropy field H_a . This is the field required to reverse all spins as one unit within a saturated crystal:

$$H_a = \frac{2K_1}{M_s}$$

K_1 is the first order constant related to the energy required to re-align the direction of magnetisation 90° from the easy axis. M_s is the saturation magnetisation of the material. Some materials have only one preferred easy axis, such as Co (figure 8). This is an example of uniaxial magnetocrystalline anisotropy.

2.1.9 Coercivity Mechanisms

Coercivity H_c is one of the most important magnetic properties of a permanent magnet. The coercivity is ability of a magnet to resist a demagnetisation force. In order to reverse the field there has to be movement of the domains. Therefore in order to be able to resist this and create a highly coercive material it is necessary to impede the motion of domains or inhibit the nucleation of reverse magnetic domains in the first place. The anisotropy defined as, the smallest applied field needed to saturate a material in the hard direction, is also the theoretical maximum value of a materials coercivity. However in practice due to the nucleation and growth of opposing domains the values are much lower. The value of coercivity can be determined by the expression:

Where $\alpha(T) \leq 1.0$, is a temperature dependant microstructural parameter, which can be enhanced by reducing the grain size and creating uniform grains. N is the demagnetisation factor¹¹

The three main extrinsic mechanisms responsible for inducing coercivity in a permanent magnet are:

- i) Domain wall pinning
- ii) Inhibiting the nucleation of reverse domains
- iii) Single domain particles

2.1.9i Domain Wall Pinning

It is possible to impede the motion of domains by adding inclusion into a material. This is demonstrated by $\text{Sm}_2\text{Co}_{17}$ materials. Magnetic inclusions can be defined as, isolated areas of a second phase material, which possess magnetic properties different to those of the matrix material. These inclusions can be found in many different forms. For example insoluble second phase material, oxides, carbides, pores, voids or cracks. The energy associated with domain walls is reduced when it intersects an inclusion present in the material. The domain walls are therefore attracted to inclusions, once the domain walls intersects it and is effectively pinned. Once pinned the coercivity of the material will increase as the amount of energy needed to move the domain walls is increased by the presence of the inclusion – domain wall intersection. In $\text{Sm}_2\text{Co}_{17}$ material presence of a $\text{Sm}(\text{Co,Cu})_5$ -rich phase, which is enclosed by a cell wall will effectively pin magnetic domains (figure 9).

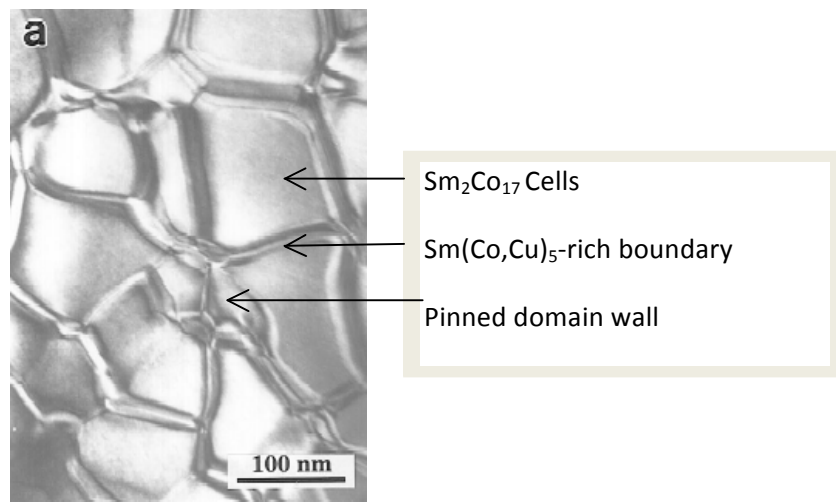


Figure 9: TEM micrograph showing the cell structure and domain wall pinning in $\text{Sm}_2\text{Co}_{17}$.

2.1.9ii Nucleation controlled mechanism

In magnets that exhibit a nucleation controlled coercivity mechanism, such as SmCo_5 - type and sintered NdFeB -type magnets. The nucleation and growth of reverse domains will create a demagnetisation field within the material and reduce its coercivity. Reverse domains can nucleate at high energy sites, such as grain boundaries with surface irregularities and incoherent precipitates. Once a reverse domain develops within the material there is no barrier

to prevent its movement throughout the grain, until it reaches another grain boundary. The best way to eliminate reverse domains is to smooth out the grain boundaries. This can be achieved by effective liquid phase sintering during the materials manufacturing. It is also favourable to avoid the presence of soft magnetic phases at grain boundaries as these can promote the growth of reverse domains across grain boundaries. Finally heat treatments can smooth out irregularities.

Figure 10 shows the initial magnetisation curve of nucleation-type materials. A characteristic steep rise in magnetisation is observed at low applied field. Here domains are aligned favourably to the direction of the applied field and grow and merge, at the expense of domains aligned opposing the applied field. The curve begins to plateau when magnetisation is hindered by the remaining reverse direction domains. These are eventually realigned to the direction of applied field, and magnetic saturation is achieved. This was discussed in section 2.1.4 domains where figure 5 showed a magnetisation curve of a sample that exhibited a nucleation controlled coercivity mechanism.

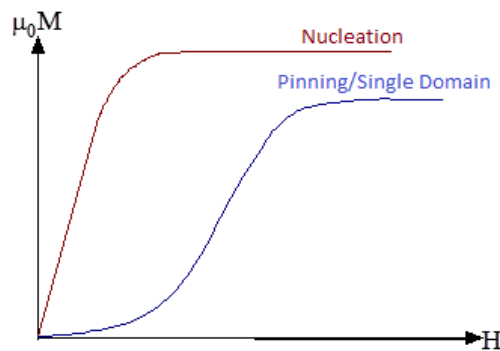


Figure 10: Magnetisation curve (first quadrant) for nucleation, pinning and single domain type materials.

2.1.9iii Single Domain

If the grain size is reduced to such a degree that only single domain grains can exist then reverse domains cannot grow and move through that structure. In order to reverse the direction of magnetisation each domain must spontaneously change direction, by uniform rotation. This requires a large amount of energy to propagate a reverse grain within a defect free material. Melt spun NdFeB magnet ribbons exhibit this type of coercivity mechanism.

2.2 NdFeB Magnets

2.2.1 Importance of Fe and Nd

NdFeB magnets have the highest energy product of any permanent magnetic material. NdFeB magnets demonstrate a high remanance due to the fact that they contain a large quantity of ferromagnetic Fe. Fe has unpaired 3d electrons, which can exhibit exchange coupling with adjacent neighbours resulting in a net magnetic moment. The high coercivity is a result of the high anisotropy demonstrated by neodymium, due to the 4f electrons.

The principal interaction in rare earth and transition metals is usually strongly ferromagnetic. In order to produce a viable Nd - Fe permanent magnet a third element is also required as there are no high Fe content Nd-Fe binary systems. When a third non-ferromagnetic element is introduced it can only be present in small quantities so as not to reduce the overall magnetic flux generated by the material.

The 1982 discoveries by both Sumitomo Special Metals Company in Japan and General Motors in the USA showed how the use of a small quantity of B as an alloying element to the Nd-Fe system led to a material with outstanding magnetic properties. This phase had the approximate composition of 12 at% Nd, 6 at% B and balance Fe. Herbst et al later identified it

as the $\text{Nd}_2\text{Fe}_{14}\text{B}$ phase¹². However each company had arrived at this discovery via different means. General motors focused on the development of a melt-spun nanocrystalline NdFeB magnet, whilst Sumitomo developed fully dense sintered magnets.

2.2.2 Phases in the NdFeB system

There have been numerous studies that have reported phase relations in the ternary NdFeB system^{13,14}. Many of these focused on the higher rare earth content commercially available alloys such as the ‘Neomax’ composition – $\text{Nd}_{15}\text{Fe}_{77}\text{B}_8$. These magnets have three main phases present; $\text{Nd}_2\text{Fe}_{14}\text{B}$ phase (Φ), $\text{Nd}_1\text{Fe}_4\text{B}_4$ (η) and a grain boundary region comprised mainly of Nd-rich material. This composition of magnet used by ‘Neomax’ is still widely used today. One of the main reasons being the high Nd content avoids the peritectic reaction at 1180°C , which produces free iron. This is shown on the phase diagram in figure 11.

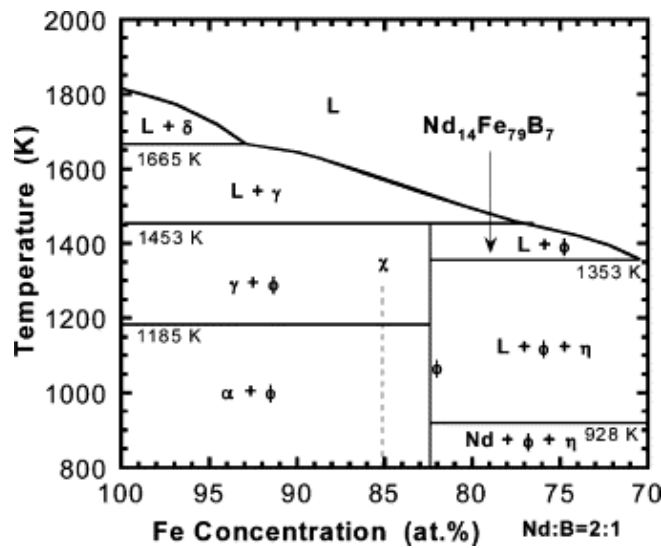
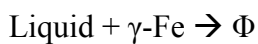


Figure 11: NdFeB phase diagram

The peritectic reaction is expressed as:



If this reaction does not fully complete then a soft magnetic α -Fe phase may remain in the final microstructure. This soft magnetic phase can severely decrease the final magnetic properties of the material and it can hinder the jet milling process which produces a fine powder.

At temperatures below 1115°C the $\text{Nd}_1\text{Fe}_4\text{B}_4$ (η) phase is formed. Below this temperature the growth of both Φ and η phases grow at the expense of the liquid phase, which finally solidifies at 655°C as a ternary eutectic.



2.2.2 The Magnetic Phase – $\text{Nd}_2\text{Fe}_{14}\text{B}$

The $\text{Nd}_2\text{Fe}_{14}\text{B}$ phase has been identified by X-ray diffraction techniques^{15,16}. A study by Herbst et al¹² showed how the crystal structure was comprised of two interpenetrating sublattices of tetragonal symmetry. Herbst et al¹² discussed the link between the crystal structure arrangement and the observed magnetic properties. The $\text{Nd}_2\text{Fe}_{14}\text{B}$ phase, demonstrates a very high degree of magnetocrystalline anisotropy. This in turn creates very high coercivity, due to the strength of reverse field required to demagnetise the material. The crystal structure for the magnetic phase is shown in figure 12.

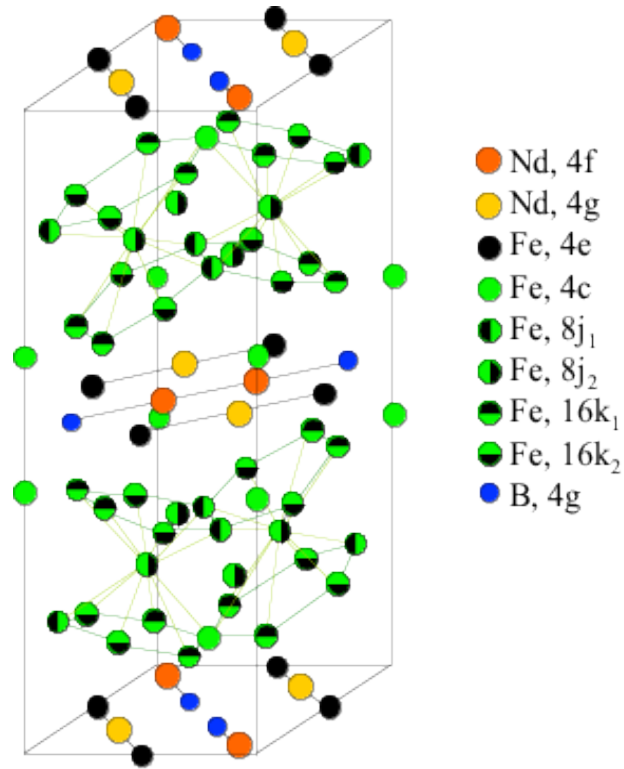


Figure 12: $\text{Nd}_2\text{Fe}_{14}\text{B}$ crystal structure diagram.

$\text{Nd}_2\text{Fe}_{14}\text{B}$ is the only ferromagnetic phase present in the NdFeB magnet. As such this phase alone is responsible for the remanence of the magnet.

2.2.3 The Nd-Rich Phase

The Nd-rich phase will typically make up around 10% by volume of the total material within the NdFeB type magnet. It has been found to play a key role in the sintering and coercivity mechanisms of the material¹⁷. During sintering at temperatures of over 1000°C the Nd-rich phase forms a liquid. This liquid aids the sintering by wetting the surrounding grains of $\text{Nd}_2\text{Fe}_{14}\text{B}$. This mechanism is the main reason for densification of sintered magnets. The Nd-rich phase is still not fully understood because of its complex structure. Hiraga et al¹⁸ identified this phase as having a bcc structure, whereas Fidler reported it was a dhcp lattice structure²⁰.

2.2.4 The NdFe₄B₄ Phase

The volume of boron present within a material will influence the amount NdFe₄B₄ phase. The NdFe₄B₄ phase is paramagnetic at room temperatures, but becomes ferromagnetic at temperatures below 25K.¹⁹ The presence of this phase within the NdFeB type magnets has no magnetic benefits and may actually be detrimental as it could act as nucleation sites for reverse grains²⁰.

2.2.4 The Nd₂Fe₁₇ Phase

The Nd₂Fe₁₇ phase can form in magnets when the B content is reduced. Due to the planar magnetic anisotropy of this phase at room temperature the magnetic field produced by Nd₂Fe₁₇ is very weak²¹. Nd₂Fe₁₇ can act as a nucleation site for the growth of reverse domains. If the phase is present in nanocrystalline grains it can form an exchange coupling interaction with the adjacent Nd₂Fe₁₄B phase, without a reduction in coercivity. However when Nd₂Fe₁₇ phase exists in the form of coarse grains or precipitates in large quantities, the coercivity of the magnet is significantly reduced¹⁴. Therefore minimising this phase during processing is essential.

2.3 Manufacturing Processes for NdFeB Magnets

The manufacturing process for NdFeB-type magnets will have a profound effect on the microstructure of the material, which will in turn, give rise to the magnetic properties. This is known as the magnetic triangle. This is only made possible as the behaviour of magnetic domains is strongly influenced by microstructure.

Since their introduction in the early 1980s many different magnet manufactures have researched processing routes, seeking the optimal conditions to make the 'perfect' permanent

magnet. There are three main production routes used to produce either fully dense or resin bonded magnets. Fully dense magnets are produced using a powder metallurgy route. Resin bonded magnets are produced by mixing nanocrystalline powders with a resin binder. Nanocrystalline powders are produced by either melt spinning or via a high temperature hydrogen processing route called HDDR (Hydrogen Disproportionation Desorption and Recombination).

The microstructure of sintered, HDDR and melt-spun ribbon produced NdFeB is shown in Figure 13

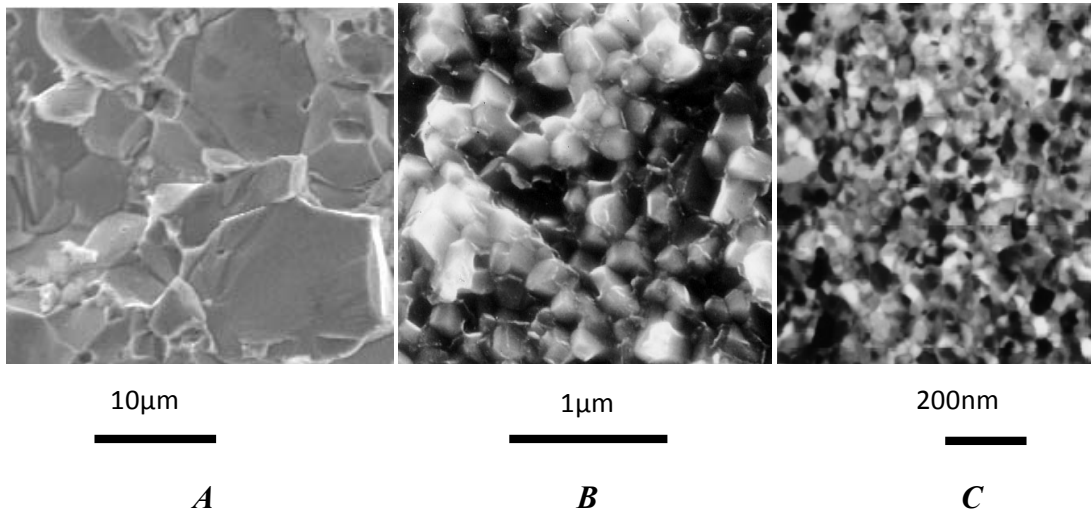


Figure 13: SEM images of A: Sintered NdFeB magnet with a grain size of $\sim 10\mu\text{m}$ B: HDDR processed material with a grain size of $\sim 300\text{nm}$ C: Melt Spun material with grain size of $\sim 20\text{-}30\text{nm}$.

2.3.1 Sintered NdFeB

To manufacture sintered NdFeB-type magnets, the raw materials are first melted in an induction furnace in elemental form at around (1400-1500°C). The molten alloy is then either poured into a book mould and cooled or onto a water-cooled rotating copper wheel in a process known as strip casting²². The cast alloy can then either be crushed and jet milled to produce fine particles or the crushing process can be avoided using a technique known as

hydrogen decrepitation. During hydrogen decrepitation the alloy breaks down to a friable powder that can be milled very easily in a jet mill. The HD process is described in more detail in section 2.3.1i

The fine particles which are produced post jet milling are aligned in a magnetic field and pressed either uniaxially or isostatically into green compacts. The green compacts are then sintered in a vacuum furnace at around 1000°C. Finally these blocks are then heat-treated, cut to shape, surface coated and magnetized to form the final product. The flow diagram of this process is shown in figure 14.

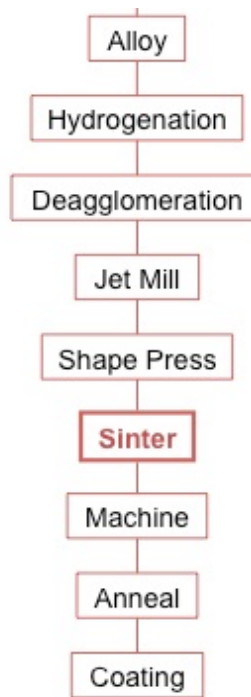


Figure 14: *Sintered NdFeB magnet manufacturing flow diagram*

The ideal microstructure would have uniform fine grains with smooth grain boundaries and a high degree of anisotropy along the c-axis. This results in a reduction in the number of nucleation sites for reverse domains, leading to very good coercivity values.

i) Hydrogen Decrepitation

One of the most efficient ways to break NdFeB alloys down into a friable powder is to use hydrogen. During the HD process hydrogen is initially absorbed by the Nd-rich phase at the grain boundaries forming $\text{NdH}_{2.7}$. This results in an exothermic reaction which allows hydrogen to be absorbed interstitially by the $\text{Nd}_2\text{Fe}_{14}\text{B}$ matrix grains, forming a solid solution. The hydriding process results in expansion of the matrix grains by around 5% which causes intergranular and transgranular cracking. It also results in the surface grains peeling away from the surface of the alloy. The HD process was developed initially for SmCo_5 alloys by Professor Rex Harris and was subsequently used for NdFeB alloys fig 15

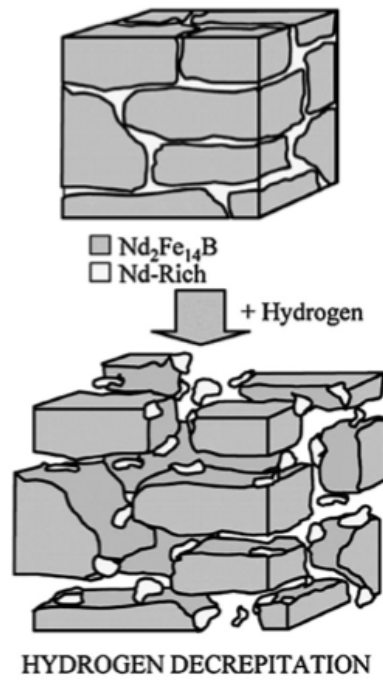


Figure 15: *Hydrogen Decrepitation schematic.*

It is believed that hydrogen is used in the production of > 90% of all NdFeB magnets today. The powder created by the HD route is very friable which leads to faster jet milling rates (figure 16). It is believed that by using hydrogen as opposed to crushing results in a 25% cost saving.²³

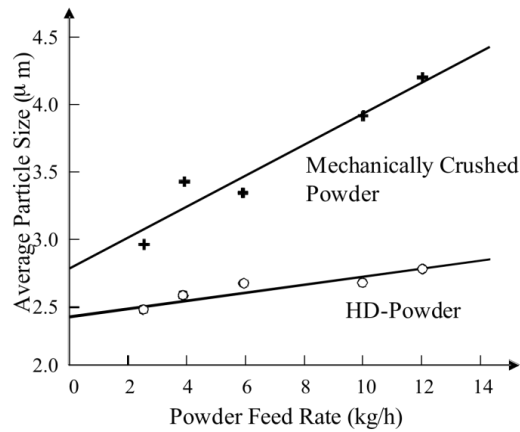


Figure 16: *Average particle size versus feed rate for HD and Mechanically crushed powder²⁴.*

2.3.2 Resin Bonded NdFeB Magnets

There are two routes to produce nanocrystalline powders that are suitable for resin bonded magnets; melt spinning and the HDDR process. Both of these routes are described below.

i) Melt Spinning

Melt spinning is a process used to produce nanocrystalline ribbons of NdFeB. Cast NdFeB is heated by an induction coil until molten (1400-1500°C). Molten alloy is ejected under a pressure of argon through a nozzle onto a water cooled rotating wheel. Upon contact with the wheel the material cools rapidly producing ribbon, typically 30µm in thickness. The rapid cooling prevents grain growth and therefore creates a homogenous fine nanocrystalline microstructure. A schematic of the melt spinning process is shown in figure 17

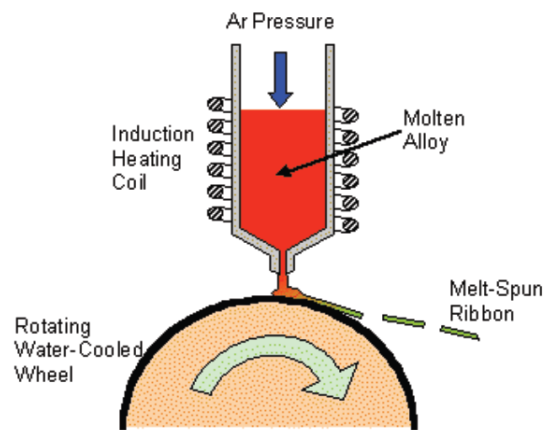


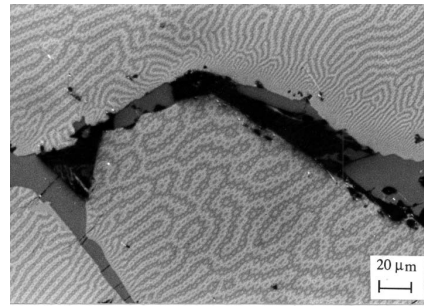
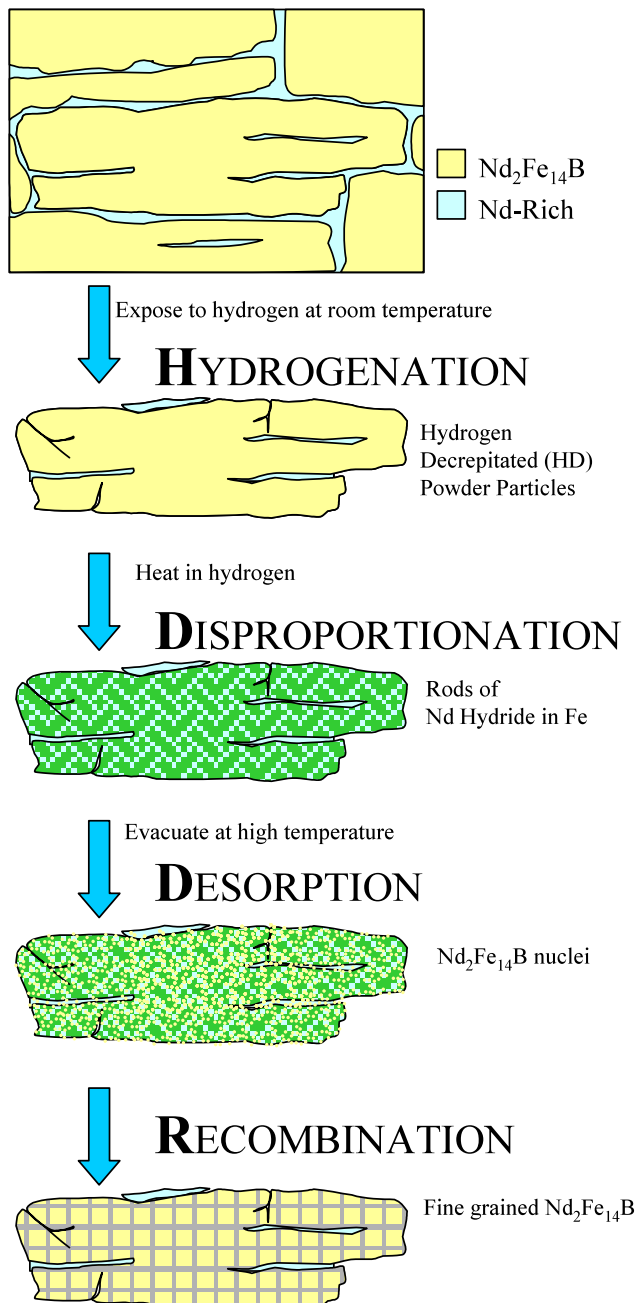
Figure 17: Schematic of the Melt Spinning manufacturing process

The melt spinning process is simple and relatively cheap. However the melt spun ribbons have randomly orientated grains, which results in isotropic magnetic behaviour. The result of this is a relatively low magnetic remanance. The coercivity mechanism exhibited by these materials is that of single domain particles, due to the very small grain size. (Section 2.1.9)

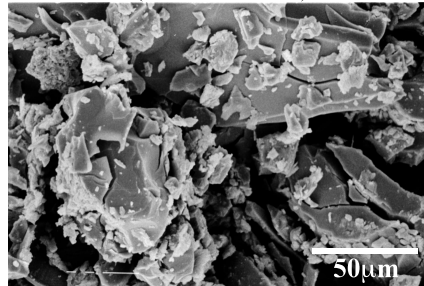
ii) HDDR

The Hydrogenation Disproportionation Desorption Recombination (HDDR) process has been used to manufacture high coercivity powders for resin-bonded magnets. This process was

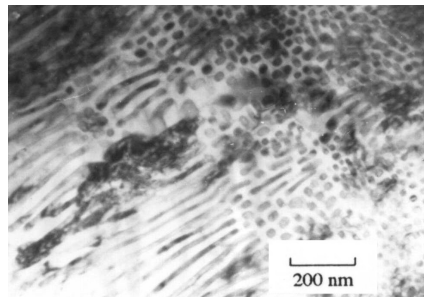
introduced in 1989 by Takeshita and Nakayama²⁵ who first reported the hydrogenation-dehydrogenation process, where cast NdFeB magnets were heated to $\sim 800^{\circ}\text{C}$ in a hydrogen atmosphere which was then evacuated. The resulting powder from this process was magnetically coercive yet isotropic in nature. Work by McGuinness et al.²⁶ described the HDDR treatment to process magnetic powder, consisting of the following steps, shown in the figure 18.



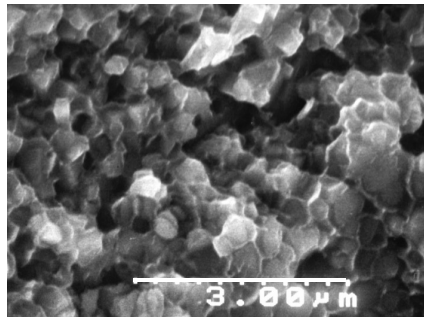
Optical Kerr Micrograph of Cast Alloy
(Domain Contrast)



SEM Micrograph of HD Powder



TEM Micrograph of
Disproportionated Material



SEM Micrograph of the Surface of
an HDDR Powder Particle

Figure 18: HDDR processing route with microstructure images.

The following process can be divided into two main reactions the disproportionation reaction (A) and recombination reaction (B):

A) Disproportionation

The first reaction that occurs when the material is heated up to 850⁰C and the hydrogen pressure is above 700mbar is known as Disproportionation. During disproportionation, the large-grained (~15µm) magnetic phase, Nd₂Fe₁₄B, reacts with hydrogen to form 3 different phases:



Hydrogen diffuses along the Nd-rich phase, in the same way it does in the HD process, then from the edges of the Nd₂Fe₁₄B phase inwards. The resultant microstructure consists of colonies of alternating NdH₂, and αFe rods. These phases have a very fine microstructure with the Nd content evenly dispersed throughout the material. The disproportionation reaction is highly exothermic.

B) Recombination

When the hydrogen pressure falls below the equilibrium point of 700mbar the recombination reaction takes place:



During recombination the nucleation of Nd₂Fe₁₄B at many points within the fine disproportionated mixture leads to a much finer Nd₂Fe₁₄B grain size (~0.3µm). Initially hydrogen will desorb from the NdH₂ phase found both in the matrix and more abundantly within the Nd-rich grain boundary area. As the temperature remains above the Nd-rich phase melting point it remains a liquid. It is believed that during the recombination diffusion of iron into the liquid phase is the rate-controlling factor²⁷. The recombination reaction is an

endothermic reaction. The drop in temperature, if significant can affect the magnetic properties of the powder.

Later studies²⁸ on HDDR processing showed how it was possible to develop anisotropic HDDR powder. This was achieved by controlling the disproportionation reaction rate using different hydrogen pressures during processing. Kwon et al²⁹ carried out a study into the effect of hydrogen pressure on disproportionation kinetics using an arc melted alloy with the composition of $\text{Nd}_{12.5}\text{Fe}_{80.6}\text{Ga}_{0.3}\text{Nb}_{0.2}\text{B}_{6.4}$. The study showed that hydrogen pressure during the disproportionation controls the kinetics of the disproportionation reaction, and this strongly influences the texture in the final HDDR-treated material. Therefore the anisotropy observed in the HDDR powder can be linked to the disproportionation reaction where $\text{Nd}_2\text{Fe}_{14}\text{B}$ decomposes into three phases: cubic NdH_2 , cubic Fe and tetragonal Fe_2B . Out of these three phases only Fe_2B has an anisotropic crystal structure. Honkura et al³⁰ hypothesized this phase may be essential to the development of anisotropy in HDDR material (figure 19). Gutfleisch described this as the texture memory effect.²

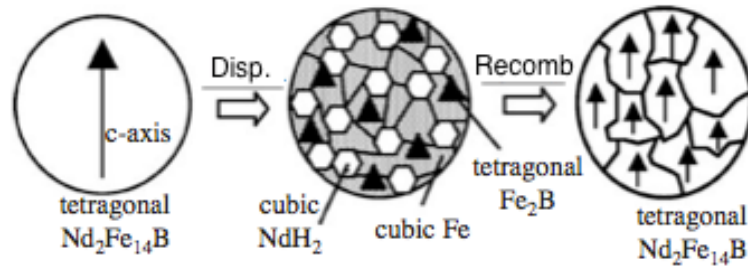


Figure 19: Adapted schematic showing structural changes throughout HDDR, with Fe_2B as hypothetical orientation site. Left: before HDDR. Middle: Disproportionated structure with aligned Fe_2B . Right: Fine grained aligned material after HDDR.

Honkura³¹ proposed that Fe_2B phase precipitated along to tetragonal $\text{Nd}_2\text{Fe}_{14}\text{B}$. During phase transformations the Fe_2B crystallites keeps the original crystal orientation of $\text{Nd}_2\text{Fe}_{14}\text{B}$ (figure 20). Therefore it is assumed that the fluctuation of Fe_2B will affect the degree of anisotropy. The fluctuation of Fe_2B is governed by the rate at which the reaction rate. Fe_2B maintains the original alignment if the reaction rate between the hydrogen and the NdFeB is low. As a result a slow disproportionation and recombination reaction will create an anisotropic HDDR powder. If these reactions happen too quickly i.e. at a high hydrogen pressure, then Fe_2B precipitates at random, leading to an isotropic HDDR powder.

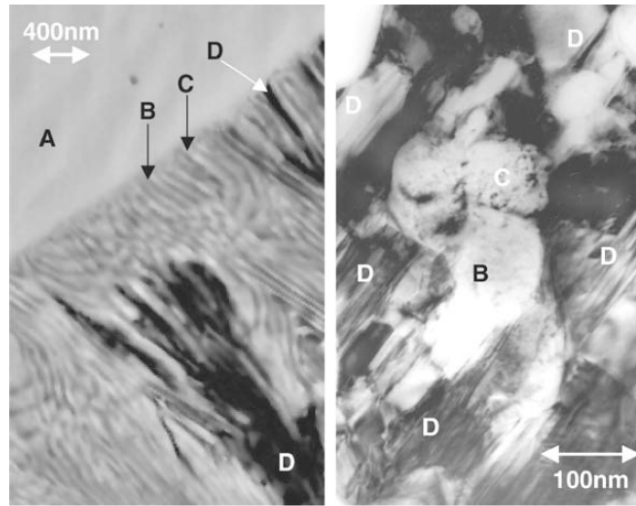


Figure 20: (Left) backscattered SEM micrograph showing the reaction front during disproportionation (Right) TEM bright field image showing well aligned Fe_2B grains within disproportionated structure. (A: $\text{Nd}_2\text{Fe}_{14}\text{B}$, B: $\text{Fe}/\text{Fe}(\text{B})$, C: NdH_2 and D: Fe_2B)

These results were backed up by work by Guth et al³¹ who carried out a study using an arc melted alloy with a composition of $\text{Nd}_{27}\text{Fe}_{\text{bal}}\text{Ga}_{0.35}\text{Nb}_{0.26}\text{B}_{1.1}$. Guth³² processed this material at pressure of 0.3, 0.5 and 1bar hydrogen at a temperature of 840°C . This study indicated that initially increasing the hydrogen pressure lead to a decrease in particle alignment until at 1bar pressure it was deemed to be isotropic (figure 21).

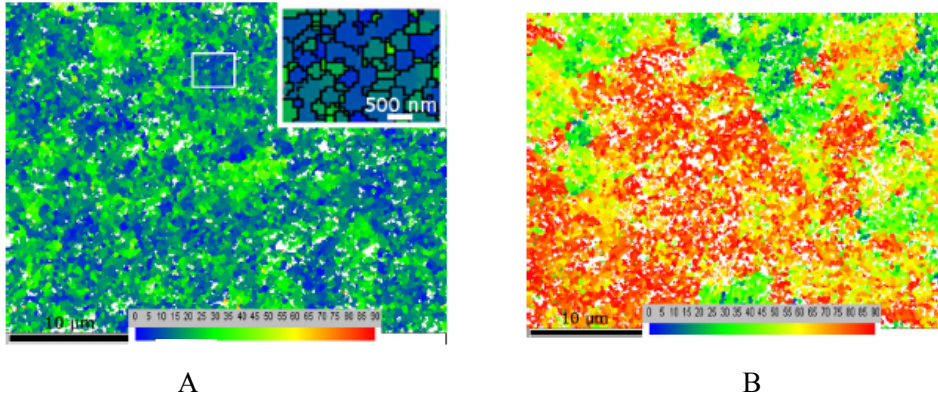


Figure 21: EBSD orientation maps showing the degree of deviation from the crystallographic $[0\ 0\ 1]$ axis for: A) HDDR powder processed at 0.3 bar hydrogen and B) HDDR powder processed at 1 bar hydrogen. From Guth et al (2011)

From figure 21 it is possible to see the material processed at 0.3 bar hydrogen had good alignment i.e. little deviation shown as a blue-green colour on the spectrum. However the material processed at 1 bar hydrogen shows little anisotropy as shown by the orange-red colour on the spectrum. The hysteresis loops for these materials are shown in figure 22.

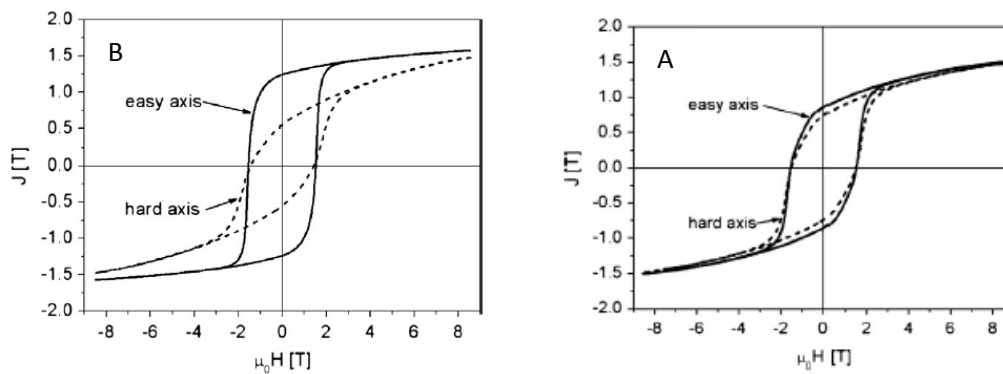


Figure 22: Magnetic hysteresis loops produced from compact aligned HDDR powder of: A) strong anisotropic material processed at 0.3 bar hydrogen and B) weak anisotropic material processed under 1 bar hydrogen.

Guth³¹ drew similar conclusions to the Honkura³⁰ postulating the mechanism by which the tetragonal Fe₂B phase maintains c-axis alignment will only work by keeping a constant low hydrogen pressure, when processing above 800°C. He noted that it is important to limit the disproportionation and recombination reaction rates by keeping as close as possible to the thermodynamic equilibrium of the phase transformation of the Nd₂Fe₁₄B and the disproportionated NdH₂ Fe₂B and α Fe phase.

2.3.5 Conventional and Dynamic Processes

Early studies on HDDR processing^{32,33} used what is known as conventional HDDR (c-HDDR) in which the cast alloy is heated in a hydrogen atmosphere up to a set temperature 850-950°C and then held for up to 2 hours, allowing disproportionation to occur. After this time, vacuum is applied rapidly which results in removal of hydrogen from the sample leading to recombination. This method has led to reasonable magnetic properties being achieved after processing however noticeably larger grains are often present alongside spherical Nd inclusions. However this route used on cast alloys only allowed for the production of isotropic HDDR powders. An alternative to this approach is known as dynamic HDDR (d-HDDR). This processing route allows hydrogen pressures and flow rates into and out of the material to be controlled allowing the processing conditions to be adjusted. The sample is heated under vacuum initially until it reaches the desired processing temperature. At this stage hydrogen can be gradually introduced into the sample at a set flow rate until it reaches a set pressure where it is held for a specific amount of time. Similarly during recombination a gradual removal of hydrogen can be achieved at a given flow rate allowing a controlled reaction to occur. This processing route has allowed anisotropic powders to be developed with good magnetic properties. Figure 23 shows the comparison between c-HDDR and d-HDDR processing routes.

The d-HDDR route is the one used in this study.

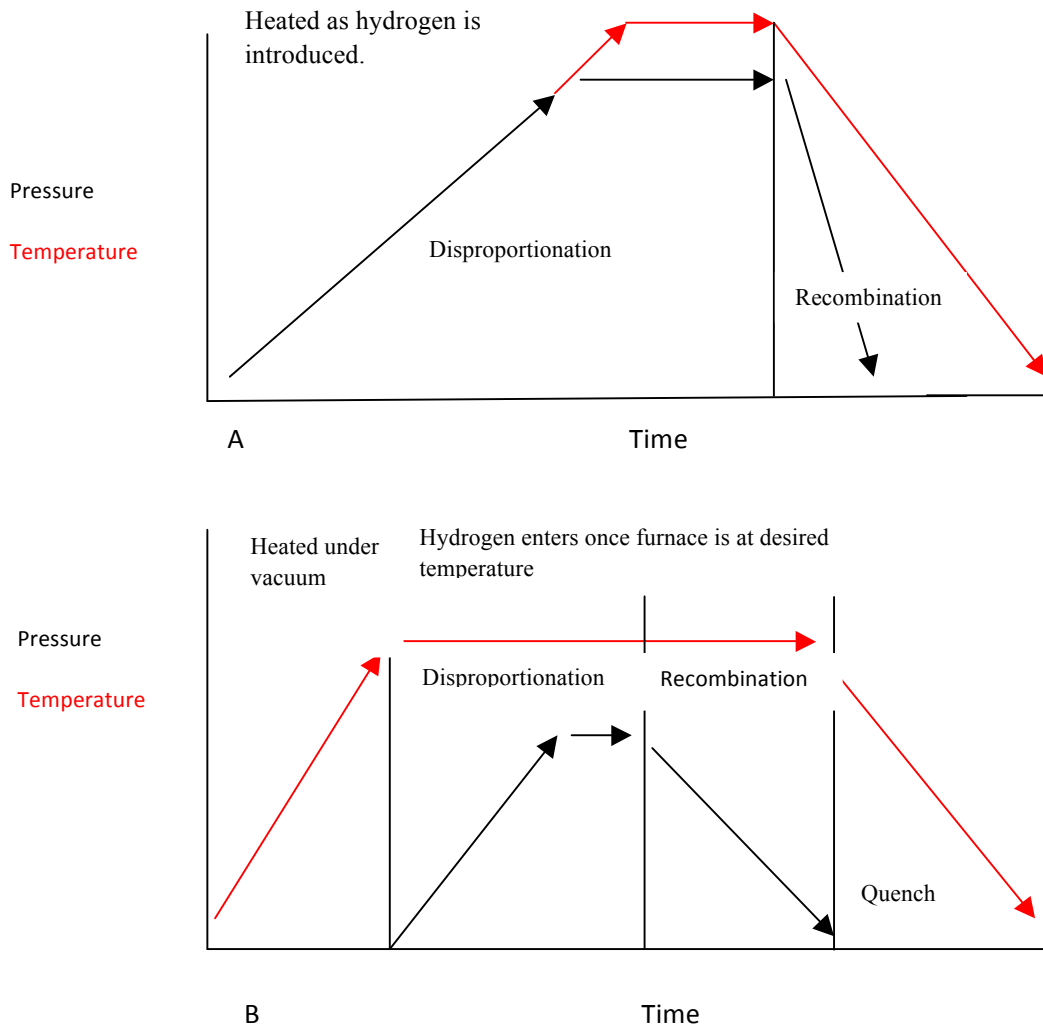


Figure 23. A diagram to show the differences between A) c-HDDR, hydrogen flow (black) and temperature change (red), and B) d-HDDR, hydrogen flow (black) and temperature change (red)

In order to achieve the best results from HDDR processing it is important to understand how the variables will alter the microstructure of the material. The temperature, hydrogen pressure,

dwelling times and ramp rates will all alter the resultant grain structure and therefore magnetic properties. It is difficult to optimise this process, as many of the variables are inter-dependant. For example a reduction in temperature will lower the equilibrium pressure at which disproportionation/recombination will take place. Even the mass of the alloy will have a large effect on many of the variables, due to the exothermicity of disproportionation and the endothermicity of recombination³⁴.

2.4 The Effect of Additives on HDDR Processing

Alloying additions are used in alloys for both sintered and bonded magnets. NdFeB-type magnets can contain a significant number of alloying additions. Therefore it is important to understand how they influence the sintered or cast magnets magnetic properties. It is also important to know what effect alloying additions will have on HDDR powder magnetic properties and the HDDR processing route. A commercial magnet can include:

Nd	29-32wt%	Fe	64.2-68.5wt%	B	1-1.2wt%
Al	0.2-0.4wt%	Nb	0.5-1wt%	Dy	0.8-1.2wt%

2.4.1 Cobalt

The addition of Co is used to improve a sintered magnets performance at high temperature Co has a higher exchange integral and thus a higher Curie temperature. This is at a cost however as the increase in Co will reduce the coercivity³⁵.

In HDDR processed NdFeB materials the effects of Co have been previously studied. Takeshita et al.³⁶ showed how the addition of Co, into cast NdFeB powder pre HDDR processing may lead to the development of a highly anisotropic powder. This powder was then formed into a bonded NdFeCoB magnet with superior magnetic properties compared to a

bonded NdFeB magnet. Takeshita³³ concluded Co was essential for the development of anisotropy within HDDR powder. This however was proved to be false as Nakamura et al.³⁷ showed it is possible to create anisotropic HDDR powder without Co, theorising that the mechanism for coercivity in HDDR powder is a selective grain growth during the recombination stage. This suggested that Co is not an essential addition to HDDR processed NdFeB type magnets in order to develop anisotropic material. A later study by Mishima²⁸ also produced anisotropic HDDR powder with strong magnetic properties without the addition of Co. Mishima³⁵ however identified that the hydrogen pressure during disproportionation and recombination is important in creating anisotropic magnet powders with good magnetic properties.

When considering the HDDR process conditions, Mishima²⁸ noted that Co does affect the pressure at which the disproportionation reaction begins. A high Co content will shift the initiation of disproportionation to a higher temperature as Co inhibits this reaction. Thus a higher pressure of hydrogen is required to start the reaction. Therefore the optimal HDDR processing conditions will alter depending on the material's Co content. i.e. different compositions may need different hydrogen pressures and temperatures to achieve optimal magnetic properties.

2.4.2 Dysprosium

Another widely used additive is dysprosium (Dy). The addition of the heavy rare earth element will noticeably improve the coercivity of the material but leads to a reduction in the remanance. The loss of remanance exhibited is due to the negative exchange coupling of Dy with the ferromagnetic iron. The optimal amount of dysprosium in a material often depends on the material's application. The cost of dysprosium is very high so it is only used when absolutely necessary in high temperature applications (typically no more than 10at%). Dy can

also improve coercivity as it slows grain growth during sintering. This limiting process creates a magnetic material with a fine grain structure.

Kim et al³⁸ created fully dense NdFeB magnets by combining additions of aluminium and dysprosium, using the sintered magnet metallurgy method. The (Nd,Dy) – (Fe-Al) B type magnet had significantly improved the magnetic properties to sintered magnets which did not contain the additions. The study concluded that compounds containing equal atomic amounts of dysprosium and aluminium lead to the best magnetic properties. The intrinsic coercivity of the alloy increases linearly with the dysprosium content at a rate of “about 7.5kOe/at % Dy.”³⁸ It is noted that in the presence of aluminium much less dysprosium is needed to reach a critical level of coercivity, thus it is cheaper and more economical to produce such a sintered magnet.

The impact Dy has on the HDDR process has been previously reported by Guth et al³⁹. Guth’s study examined recycling sintered NdFeB type magnets using the HDDR process. The study reported that the presence of Co and or Dy lead to stabilisation of the (Nd,Dy)₂Fe₁₄B phase against disproportionation. Guth concluded additives like Co and Dy shift the optimum hydrogen pressure for highest texture quality to higher values. This means that the required hydrogen pressure to initiate disproportionation of materials containing quantities of Dy will be increased.

2.4.3 Aluminium

The presence of aluminium is inevitable in all commercially produced NdFeB-type magnets, as the production of boron creates Al impurities in the material. Aluminium is widely used with cobalt additions as previously described.

In sintered NdFeB magnets, Al addition combined with the Co presence increased the coercivity due to the formation of non-magnetic Laves phases, $\text{Nd}(\text{Fe},\text{Co})_2$, in the grain boundaries. An addition of approximately 10at% Al can enhance the coercivity of sintered magnets. However the presence of aluminium itself in the matrix “reduces the intrinsic magnetic properties of the magnetic ϕ phase ($\text{Nd}_2\text{Fe}_{14}\text{B}$)”⁴⁰. This is due to the substitution of Fe with the Al element in the matrix phase⁴¹

Knoch et al ⁴² described the presence of an Nd(Fe-Al) phase present on the grain boundaries of sintered magnets. During sintering and heat treatment processes of these magnets the presence of aluminium has been shown to decrease the wetting angle³⁸. This better wetting allows a more even distribution of Nd-rich phase throughout the material as well as producing an even distribution of grain boundary material.

A study into the effect of Al on the HDDR process by Galego et al⁴³ suggested that small amounts of Al stayed in the matrix phase and acted as nucleation sites to induce anisotropy. However the study noted that in the grain boundaries Al may act as a reverse domain nucleation region.

2.4.4 Copper

The effect of copper on NdFeB has been investigated widely over the years. The use of Cu was first reported by Shimoda et al⁴⁴. The study noted there was no copper present in the matrix phase of a cast magnet. It instead enters into the grain boundaries of the material where it forms $\text{Nd}_{30}\text{Fe}_{65}\text{Cu}_5$ which has a profound effect on the coercivity of the magnet⁴⁵. The addition of 1.5% copper in to sintered magnets has been shown to provide the best magnetic

characteristics. This addition provides two beneficial effects; it reduces the grain size of the as-sintered material and alters the composition of the phases present in the material⁴⁵.

However in a sintered magnet with a composition of $\text{Nd}_{17}\text{Fe}_{76.5}\text{B}_5\text{Cu}_{1.5}$ it was found that without heat treatment it exhibited a poor coercivity. Kianvash et al⁴⁶ carried out a study into the effect of heat treatments on this composition. TEM imaging and analysis identified the presence of an $\text{Nd}_2\text{Fe}_{17}$ phase which is soft magnetic. A two stage heat treatment consisting of 1100°C for 1 hour and quench followed by 600°C for one hour and quench was proposed³³. Post treatment microstructural analysis showed the removal of the soft magnetic $\text{Nd}_2\text{Fe}_{17}$ phase and formation of copper containing phases at grain boundaries. The removal of $\text{Nd}_2\text{Fe}_{17}$ leads to improved coercivity in the sintered magnets, compared to magnets that did not contain Cu.

Additions of less than 1at% Cu can lead to improved coercivity when mixed with other additions such as cobalt and dysprosium. Research by Ragg and Harris⁴⁷ found that the addition of 0.25at% copper content to hydrogen decrepitated powder resulted in an improved intrinsic coercivity without the expected loss of remanance. If then followed by a heat treatment and rapid quenching of the sample then better properties can be achieved.

2.4.5 Niobium

Another commonly used addition by many sintered magnet manufactures is niobium. The benefits of this addition are that even a few at% Nb can improve the ‘squareness’ of the hysteresis loop. This is because Nb increases the anisotropy of the material in the same way as Dy, by negative exchange coupling. Niobium will reduce the remanance of the magnet⁴⁸. The addition of Nb to NdFeB magnets will boost its performance at higher temperatures⁴⁹.

A disadvantage to the addition of Nb can be the formation of the $\text{Nd}_2\text{Fe}_{17}$ phase in the same way as the addition of Cu. This leads to a decrease in the sintered magnet's coercivity. Further heat treatment is needed to reduce the presence of the $\text{Nd}_2\text{Fe}_{17}$ phase from the material. Allibert⁵⁰ suggested that the effect of niobium was one purely of microstructural effects. The presence of Nb containing precipitates could alter the grain growth kinetics of the $\text{Nd}_2\text{Fe}_{14}\text{B}$ grains during sintering in two different ways; by hindering coalescence, and affecting the dissolution-precipitation process. This reduction in grain coalescence was observed by Rodewald and Wall⁵¹ who carried out a study showing the addition of Nb leads to a reduction in the average grain size of the material. As with many additions the decreased grain size is responsible for the improvement in coercivity.

Galogo's⁴³ study into the effect of Nb additions on HDDR PrFeB based materials stated. "The reasonable coercivity in the Nb-containing HDDR magnets was attributed to the effect of Nb on refining of the magnetic grains, in the same way as is observed in studies carried out on sintered magnets."

2.5 The Effect of Oxygen Content on HDDR Processing

Oxygen content is another important variable to be aware of when processing a powder via the HDDR route. The oxygen content will vary depending upon whether the starting material is book or strip cast NdFeB or a final sintered magnet. It is believed that the presence of oxygen in the material can have a similar effect as that of alloying additions in terms of its effect on HDDR. Many alloying elements including cobalt and dysprosium lead to a greater hydrogen pressure before disproportionation initialises.

Corfield et al⁵² carried out work into sintering of permanent magnets. The study noted the influence of oxygen on grain growth in rare earth sintered magnets, both Pr-Fe-B and Nd-Fe-

B. In low oxygen content rare earth magnets there was excessive grain growth on sintering. When the oxygen content was increased this resulted in the elimination of abnormal grain growth in the rare earth magnet upon sintering. The study concluded a progressive decrease in oxygen content of the material resulted in a change in the intrinsic coercivity. The magnets that showed no effect on grain growth had between 1500-1600ppm of oxygen but at high oxygen contents (>3350ppm of oxygen) the grain growth rate slows. This suggested that oxides form and act as an inhibitor for grain growth during sintering. The oxygen is concentrated in the Nd-rich phase, which forms a liquid on sintering. Oxygen can alter the interfacial energy or interfacial dissolution and re-precipitation steps during the liquid phase sintering⁵³.

However if the oxygen level is too high then the material will not sinter effectively as the Nd-rich phase does not form a liquid at the normal sintering temperature. This leads to porosity and a reduction in the coercivity of the magnet. As the HDDR process relies on melting of the rare earth content of the material and redistributing it evenly throughout the bulk of the Nd₂Fe₁₄B phase it is important to understand the effect of oxygen on grain growth, especially when desiring an end product with fine even shaped grains.

2.6 Hydrogen Recycling Techniques for NdFeB Magnets

Many previous studies into HDDR processing focused the use of cast alloys as the starting material. However with a growing level of scrap magnet available on the world market and due to the price rise and volatile nature of the rare earth industry, there has been a push towards recycling of sintered NdFeB magnets. Over the last 10 years the University of Birmingham has carried out many studies into hydrogen recycling techniques of sintered scrap magnets. There are a number of challenges to overcome when recycling NdFeB from scrap sources. These challenges start with identifying, sorting and collecting devices

containing NdFeB. Then being able to separate the NdFeB material from the device. Lastly purification and reprocessing methods need to be developed to create new magnets with desirable properties.

2.6.1 Separation and Extraction Techniques

The main source of scrap magnet used by the University of Birmingham comes from computer hard disc drives. This is due to the ease of availability as they are already removed and collected from computers to destroy the data on the disc. Also as discussed in earlier sections hard disc drive motors are the largest single application of sintered NdFeB type magnets.

One of the biggest problems regarding the removal of NdFeB from hard disc drives is how to extract the material. Manual extraction would be a time consuming process as the casing is screwed closed and the magnets are Ni coated, glued into position and strongly magnetic. One method outlined by Walton et al⁵⁴ involved cracking open the hard disc drive using an industrial cropper then distorting the assembly with a uniaxial press. This process caused the brittle NdFeB to fracture into several pieces and split the Ni coating allowing hydrogen decrepitation at room temperature. By cutting the HDD's it concentrated the NdFeB content and allowed a route out for the hydrided powder. The study used a hydriding vessel with a rotating porous drum, which was loaded with 10 cropped and distorted HDDs. Hydrogen processing was carried out at 2bars for 2 hours, after which time the porous drum was rotated and the hydrided powder was liberated and collected at the bottom of the vessel. The study noted that most of the material had been removed from the HDDs in the first five minutes. Final purification was carried out by mechanical sieving of the material to remove impurities i.e. Ni coating or casing pieces. The Ni impurity level was shown to be less than 350ppm.

2.6.2 Reprocessing Routes

One of the most efficient recycling routes would be to use the hydrided NdFeB alloy to produce new sintered magnets. Previous work by Zakotnic et al⁵⁵ carried out an investigation into re-processing of sintered NdFeB magnets from hydrogen decrepitated scrap material. A variety of milling processes were studied before re-sintering the powder into fully dense magnets. By processing via this route it is possible to recover up to 90% of the magnetic properties of the starting magnet⁵⁶. One disadvantage of this route is the increase in oxygen content likely due to the processing route. Zakotnic et al⁵⁵ carried out a study where hydrogen processed sintered magnets were roller milled then sintered into a powder to form a fully dense magnet. The powder was milled 4 times, with each milling cycle leading to a fall in the sintered magnets coercivity. Chemical analysis undertaken had confirmed oxidation of the Nd-rich phase and loss of Nd by evaporation.

There are a number of other processing routes for which hydrogen decrepitated powder can be used (figure 24). The chosen route will depend upon the magnetic properties required by the final magnet i.e. the final magnet's application and the compositional variation of the scrap magnet feedstock⁵⁴

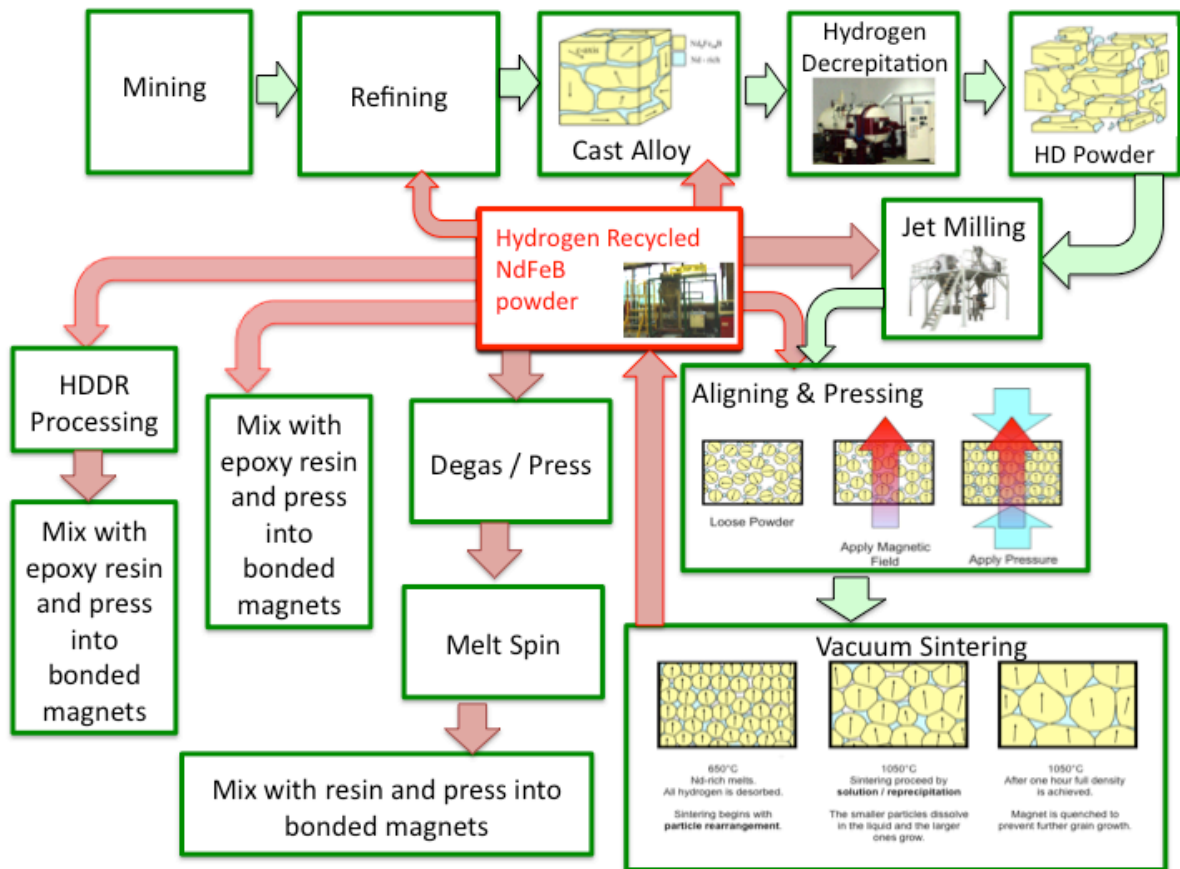


Figure 24: A schematic diagram of possible NdFeB-type magnet reprocessing routes.

2.6.3 Recycling using the HDDR process

The HDDR process is an attractive means of recycling sintered scrap NdFeB type magnets for several reasons. Firstly it can lead to improved coercivity of the material due to the fining of the grain size. The HDDR process can achieve fine grained particles (200nm-500nm)⁵⁴. A finer grain structure also leads to improved thermal stability and corrosion resistance. Corrosion is an important consideration when using rare earth magnets, as they are highly reactive. In a large grained magnet corrosion of a single grain results in a large loss of material and demagnetisation of the entire grain. In a fine grained HDDR microstructure, if a grain is exposed to corrosion and loses magnetisation, it accounts for only a small loss in volume of the material. Therefore this small loss only leads to a small decrease in the overall magnetic properties of the material.

Previous studies into HDDR processing routes for scrap magnets undertaken at the University of Birmingham have shown that it is possible to effectively re-process scrap material into new bonded magnets. Recent work by Sheridan et al⁵⁷ demonstrated that for a particular composition ($\text{Nd}_{13}\text{Fe}_{78}\text{Al}_{0.7}\text{Dy}_{0.8}\text{B}_{6.3}$) of sintered scrap magnet it is possible to adjust the HDDR processing conditions to an ‘ideal’ set of parameters, in terms of hydrogen pressure, flow rate and temperature. A slow flow rate of hydrogen into the material is believed to allow time for the disproportionation reaction reach completion, without loss of material. Similarly a slow removal of hydrogen during the recombination will allow the material time to fully process. However if done too slowly the material can be over-processed and lose its magnetic properties. The processing route outlined by Sheridan⁵⁷ is used as a template in this study as it has been shown to yield good magnetic properties (see figure 25).

The flow of hydrogen into or out of the material will determine when either the disproportionation or recombination reaction takes place. The flow rate of hydrogen is recorded during the HDDR process and can be plotted against time to generate a curve, known as the disproportionation curve. Sheridan et al⁵⁷ showed that it is possible to use the disproportionation curve to understand when the reaction initiates and completes. By understanding the shape of the disproportionation curve it is thus possible to understand what is happening to the material, as it is being HDDR processed.

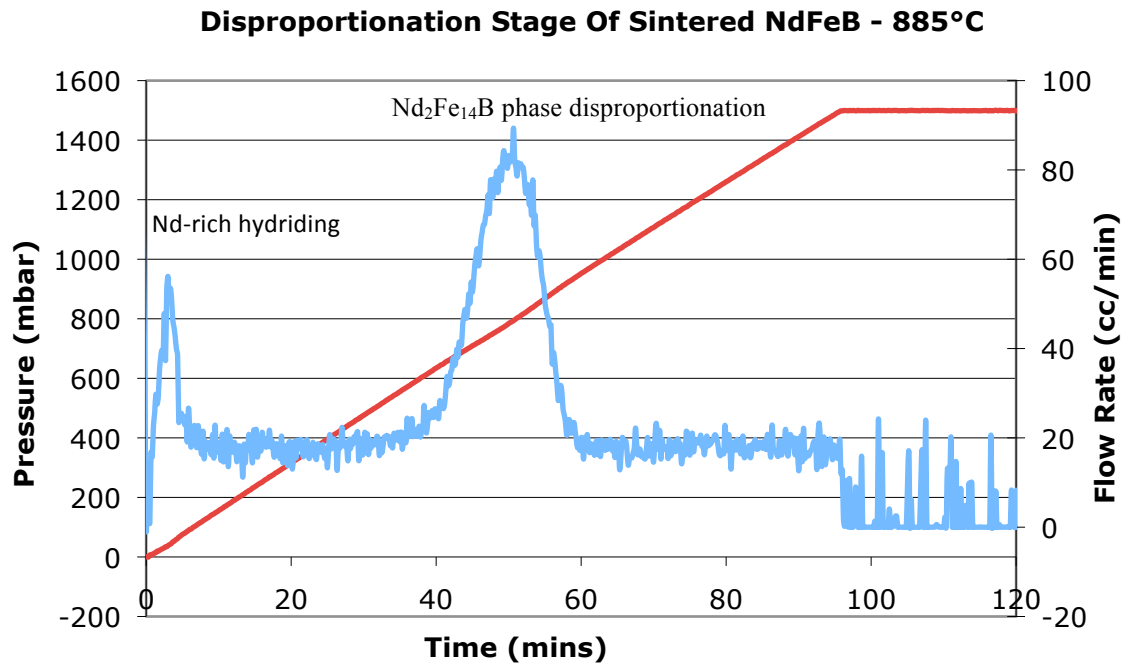


Figure 25: Disproportionation curve showing H flow rate into the material (blue) vs H pressure (red). Processed at 885°C ⁵⁷.

Sheridan et al⁵⁷ showed that an initial distinct sharp peak is observed with increasing hydrogen pressure as the Nd-rich phase hydrides at around 100mbar. Then the $\text{Nd}_2\text{Fe}_{14}\text{B}$ phase disproportionates at pressures above 700mbar at a temperature of 885°C (figure 25). It can also be observed that for this material the disproportionation reaction is completed in approximately 20 minutes. All reactions were completed within the time frame chosen in this experiment (120 minutes). The study by Sheridan et al⁵⁷ showed how it is possible to reprocess one particular sintered scrap magnet. However when considering recycling a wide range of scrap magnets with different compositions (section 2.4) and microstructures are likely to be used as the feedstock.

When considering HDDR processing the rate of reaction is dependant on the rate of hydrogen flow into the material. Hydrogen enters the material along grain boundaries using the Nd-rich areas as a highway into the material. The hydrogen then enters the matrix material from the grain boundaries inward through the $\text{Nd}_2\text{Fe}_{14}\text{B}$ phase. Therefore it is anticipated that book

mould cast material with a larger grain size (100-300 μ m) will require a longer HDDR processing time. Alternatively sintered NdFeB, which has a grain size of approximately 10 μ m, may process faster. Furthermore if processing melt spun ribbons material which has a microstructure even finer with grain size of 20-30nm this process would be expected to happen even faster.

This research project is one of many being undertaken at the University of Birmingham to understand the HDDR process and its use as a recycling method for scrap NdFeB-type magnets. The aims of this project are to examine the effect of composition, microstructure and oxygen content of scrap magnets on HDDR processing conditions and final magnetic properties. Scrap sintered NdFeB magnets are likely to have a range of compositions determined by their particular applications. Therefore it is important to investigate the effect of composition on the HDDR process. The microstructure of the scrap material will also change based upon whether the scrap material is cast scrap or sintered magnets, and also based upon the quality of the sintered magnets being used. This study will create materials with exaggerated large grains to see how this affects the HDDR processing route. Most scrap feed will fall in the spectrum between these abnormally large grains and sintered material. Finally the oxygen content of the material will be investigated. This will vary depending on how the scrap material was processed; sintered magnets will have a lot higher oxygen content than cast materials.

Experimental Procedure

3.1 Starting Materials

In this study the following magnetic materials were chosen due to their ready availability and use in previous studies⁵⁷. The rectangular Chinese sintered block was selected as the magnet to have the microstructure altered by heat treatment. The Phillips sintered magnet is used in HDD's and was selected to draw comparisons between the Chinese sintered block. Lastly cast blocks with varying Nd content were chosen to investigate the impact of altering a materials composition. Each of the starting materials underwent Inductively Coupled Plasma (ICP) compositional analysis. The results are shown below:

1) Rectangular Chinese Sintered Block- ICP= $\text{Nd}_{13}\text{Fe}_{78}\text{Al}_{0.7}\text{Dy}_{0.8}\text{B}_{6.3}$

2) Philips Sintered Magnet- ICP= $\text{Nd}_{13}\text{Fe}_{77.8}\text{Al}_{0.7}\text{Dy}_{0.6}\text{B}_{6.4}$

3) Low Rare Earth Cast Block- ICP= $\text{Nd}_{13}\text{Fe}_{78}\text{Al}_{0.4}\text{B}_{7.4}$

4) High Rare Earth Cast Block- ICP= $\text{Nd}_{15.6}\text{Fe}_{75}\text{Al}_{0.7}\text{B}_{8.2}$

3.2 Heat Treatment

In order to change the grain size of material 1 the sintered magnet was arc melted at $\sim 1500^{\circ}\text{C}$ in an argon atmosphere to create a molten “button”, which upon quenching would develop large cast grains. To homogenise the arc melted material an annealing heat treatment was performed. A study by Zhang et al⁵⁸ examines the use of various homogenisation temperatures ranging from 800°C to $\sim 1060^{\circ}\text{C}$ with varying dwell times depending on the temperature used. The study notes that 1150°C is the point at which the $\text{Nd}_2\text{Fe}_{14}\text{B}$ phase melts. Zakotnic⁵⁵ noted a loss of material when homogenising at 1080°C for 1 hour. In order

to minimize the loss of Nd a temperature of 1000°C was chosen based off previous papers^{55,58}. A time of 10 hours was selected as diffusion of Nd happens faster closer to the melting point. This time frame should be sufficient to effectively process the material.

3.3 Hydrogen Decrepitation

Initially the NdFeB-type magnets underwent hydrogen decrepitation to break down the bulk starting materials. This is necessary as the HDDR process works optimally when processing a powder. Hydrogen decrepitation was achieved by preparing a 25 gram sample of each starting NdFeB material and placing it inside a stainless steel vessel inside a vacuum furnace. The vessel was then evacuated using a standard Edwards 2-stage rotary vacuum pump to remove oxygen to an ultimate vacuum of 10^{-2} mbar. Once this vacuum was achieved hydrogen was admitted into the chamber at a rate of 100 mbar per minute up to a hold pressure of 2 bar hydrogen. This was then held at pressure for a time of 1 hour to allow the sample to effectively decrepitate. The hydrogen was then gradually removed with the use of mass flow controllers and finally by opening the chamber to a vacuum valve removing the hydrogen at 100 mbar per minute.

The decrepitated sample was then removed from the vacuum vessel and hand milled in a pestle and mortar to break apart any large particles of powder and agglomerates, creating a homogenous sized HD powder ready to be HDDR processed.

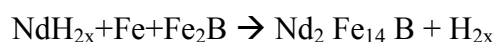
3.4 HDDR

A 25 gram sample of HD powder was loaded into a stainless vessel inside of a steel furnace tube. This was then attached to the HDDR rig and evacuated using a rotary pump to 10^{-2} mbar. The sample was then heated at 15°C per minute up to 855°C and a heating rate of 5°C per minute was used until the hold temperature of 885°C was achieved. It is at this temperature that the desorption / degassing of the material will occur and it happens from various phases below this temperature.

Once at 885°C the vacuum pump valve was closed and disproportionation was carried out. Hydrogen was admitted into the HDDR rig at a rate of 16 mbar per minute up to a hold pressure 1500 mbar, and held for 30 minutes, giving a total processing time of 2 hours. This slow rate and long processing time would allow for a variety of samples with different microstructures and compositions to fully disproportionate. These pressures and temperatures were based on previous work carried out at the University of Birmingham by Sheridan et al.^{59,60}

In the final stage of the experiment the recombination reaction takes place. Hydrogen is removed from the HDDR rig at a rate of 100 mbar per minute down to ambient pressure, using a mass flow controller, at which point the vacuum pump is engaged in order to re-establish a vacuum. The furnace is then rolled off and the sample is quickly air cooled and left under vacuum. Once again a slow decrease of hydrogen pressure during recombination will allow a range of magnets to be processed successfully using a single set of parameters.

The recombination reaction which takes place is:



Once this stage is complete the HDDR powder is removed from the HDDR rig and is ready for testing.

3.5 Testing Magnetic Properties

In order to quantify and measure the properties of the HDDR processed powder a LakeShore 7300 Series Vibrating Sample Magnetometer (VSM) was used. A small quantity of HDDR powder (~50-100 mg) was hand milled in a pestle and mortar. This was placed into a sample

holder where wax was added and then the sample holder was sealed. The entire sample holder was then placed in boiling water to allow the wax to melt and mix with the powder. The 'hot' sample holder was then placed in a permeameter and subjected to a 1.5T field for 2 minutes to align the sample. The wax cooled and hardened which maintained alignment in the "Easy" direction. The solidified sample was then pulse magnetised at 6T using a capacitor discharge pulse magnetiser.

The sample was loaded into the VSM and a program was executed to measure the magnetic properties in order to produce a hysteresis loop for evaluation. The VSM program used executed the following operation:

Ramp up from 0T to a max field of 2T taking 2 data points, Ramp down from 2T to 0T taking 10 data points i.e. every 0.2T

For the demagnetisation curve ramp down from 0T to -1T taking data points every 10 data i.e. every -0.1T, Ramp down -1T to -2T taking 5 data points i.e. every -0.2T

3.6 Microstructure Analysis

A small amount of HDDR processed powder was added into a sample mounting machine along with ground conducting bakelite. The sample was then polished using $\frac{1}{4}$ micron diamond paste on selvyt cloths. The microstructure of the material was assessed using a Leica optical microscope with the use of polarising lenses in order to produce Kerr effect images of the material. This allowed estimates of domain and grain sizes to be obtained. Imaging software was used to provide scale bars and enhancement of images for clarity.

Scanning electron microscopy was also carried out on each bakelite mounted sample using standard SEM techniques. The SEM used was the Joel 6060 with low vacuum capabilities, in backscattered mode; with a working distance of 10mm. EDS analysis was undertaken on different phases to determine their composition.

Results and Discussion

The aim of this project is to investigate the effects of altering the microstructure and composition of starting scrap magnet feedstock on the HDDR processing technique. This was achieved in the following way. Firstly an experiment into the effect of changing the microstructure of the starting material and its effect on HDDR processing is shown in section 4.1 then an experiment into sintered magnets with similar compositions, investigating recombination rates (section 4.2). Finally a brief look into the effect of increasing Nd content of cast magnets on HDDR processing. (section 4.3)

4.1 The effect of microstructure on HDDR processing

In this section the aim of the project was to investigate the alteration of grain size and phase distribution on HDDR processing. To be able to control variables such as varying oxygen content, alloying additions and differences between different types of magnet. A magnet with a known composition and starting microstructure was selected. Then the grain size was altered, via different heat treatments.

The magnet selected had a composition of $\text{Nd}_{13}\text{Fe}_{78}\text{Al}_{0.7}\text{Dy}_{0.8}\text{B}_{6.3}$ and was manufactured by a conventional powder-sintering route. This magnet is the same that was used by Sheridan⁵⁷ so is known to process well under the selected HDDR conditions.

An arc melting heat treatment was then carried out to alter the grain size of the sintered magnet. At a temperature of 1500°C the sintered magnet melted and was then was left to cool. This should encourage the development of larger grains, comparable to that of a cast material.

The arc-melted button was then annealed at the chosen temperature of 1000°C for 10 hours. The annealing process should further alter the microstructure by re-distributing the Nd-rich phase, but more importantly it should remove the presence of any free iron. The HDDR process was carried out on each of the different materials i.e. sintered, arc melted and annealed.

4.1.1 Microstructural analysis of starting materials

A scanning electron microscope in backscattered mode, supplemented with optical microscopy and Kerr effect imaging, was used to investigate the microstructure and composition of the starting NdFeB material. In this experiment the starting materials are:

- A) Sintered magnet with a composition of $\text{Nd}_{13}\text{Fe}_{78}\text{Al}_{0.7}\text{Dy}_{0.8}\text{B}_{6.3}$.
- B) Arc melted material with a composition of $\text{Nd}_{13}\text{Fe}_{78}\text{Al}_{0.7}\text{Dy}_{0.8}\text{B}_{6.3}$.
- C) Arc melted then annealed material with a composition of $\text{Nd}_{13}\text{Fe}_{78}\text{Al}_{0.7}\text{Dy}_{0.8}\text{B}_{6.3}$.

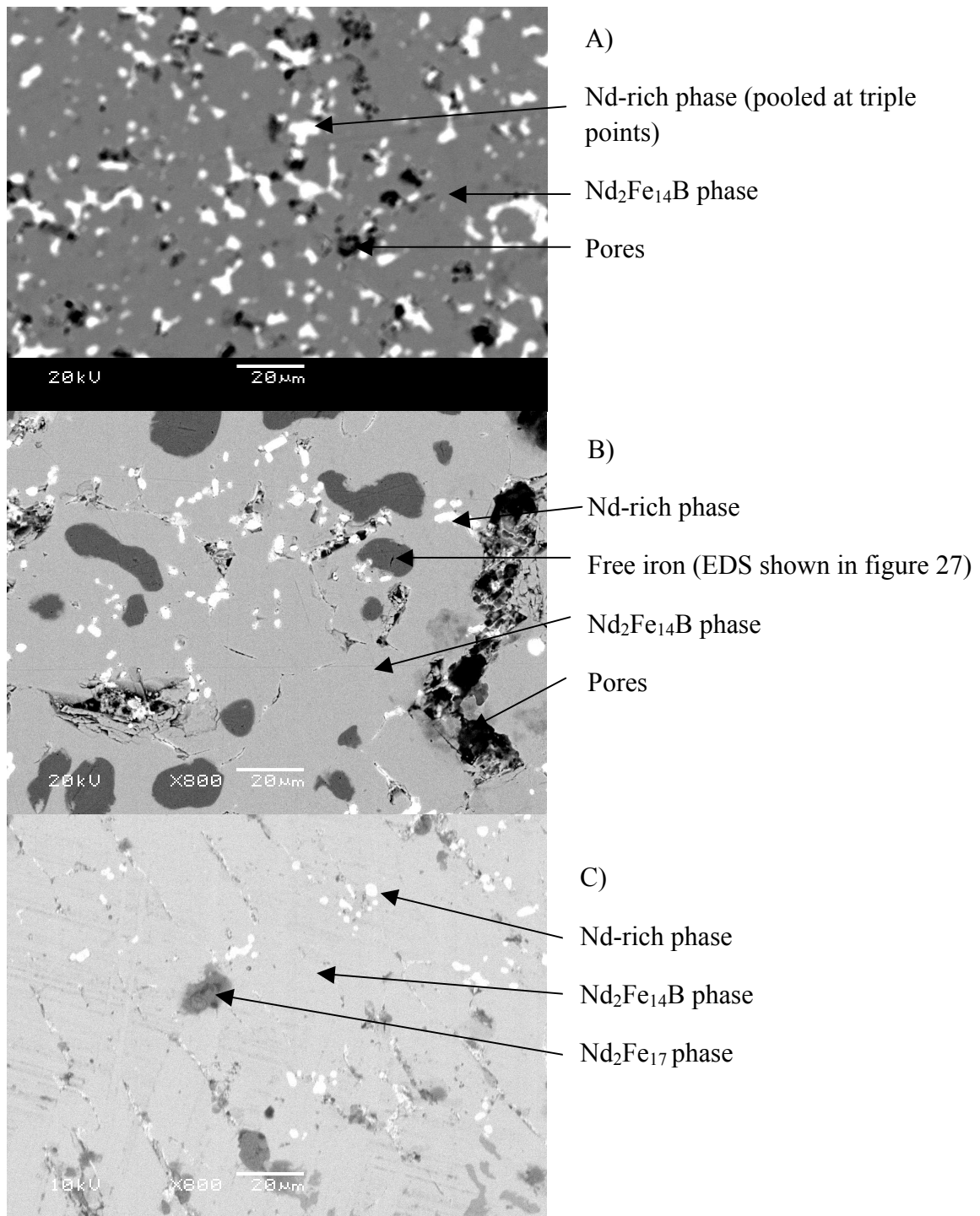


Figure 26: SEM backscattered image of: A) starting sintered magnet. B) Arc melted NdFeB material and C) Arc melted and annealed NdFeB material.

A) The backscattered scanning electron image that is shown in figure 26 A. shows a typical sintered magnet microstructure. The fine grain structure has dispersed amounts of Nd-rich phase which forms at grain boundary triple points. This magnet has no

visible free iron or other non-magnetic phases present. Thus the magnetic properties of this magnet are very good. The starting sintered magnet has a remanence of 1.36T, a coercivity of 860kA/m and a maximum energy product (BH_{\max}) of 340kJ/m³. There are some small pores present which may have occurred during sintering as the magnet solidifies or they may be a result of pull out of the Nd-rich phase during polishing.

B) Backscattered SEM images of the arc melted material are shown in figure 26 B. It can be observed that the arc melting process resulted in significant grain growth. During grain growth large regions of Nd-rich were forced into the grain boundary areas, where the Nd-rich phase is pooled. An increase in the Nd₂Fe₁₄B phase grain size would be expected to lead to a slow and lengthy disproportionation stage during HDDR processing.

Large quantities of free iron (α -Fe) could also be observed within the material. The large quantity of free iron (figure 27) will significantly affect the magnetic properties of the material. α -Fe is soft magnetic and will reduce the observed coercivity of the material. Secondly the growth in the α -Fe phase indicates a reduction in the Nd₂Fe₁₄B phase. The free iron is known to form by a peritectic reaction. This can be prevented by rapid cooling using the strip casting process. Lastly there are noticeably large pores present within the material that occurred during solidification of the material from the liquid melt.

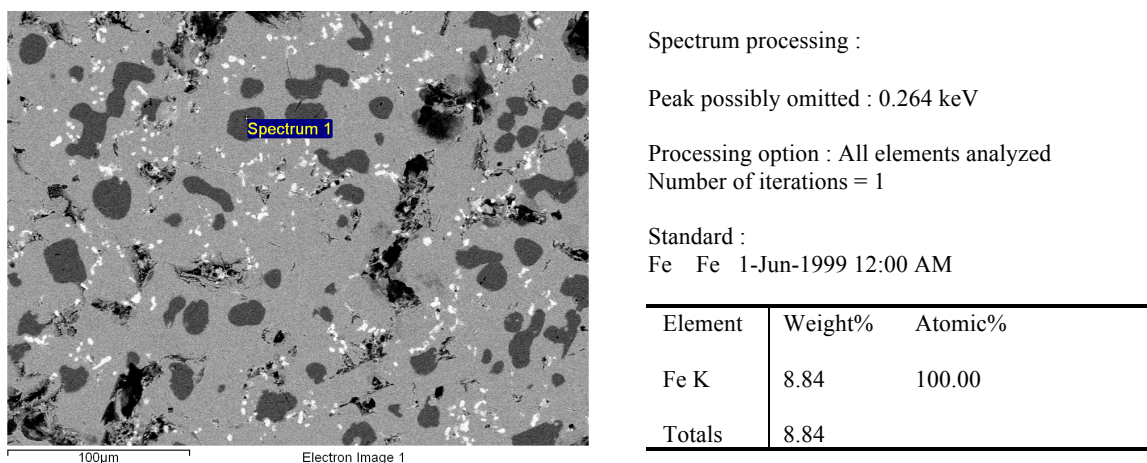


Figure 27: Backscattered SEM image with EDS analysis confirming the presence of free iron within the arc melted material.

C) Back scattered SEM images of the arc melted then annealed material are shown in figure 26 C. The annealing was selected as an effective way of removing free iron from within the material. The removal of any free iron within the material leads to an increase in the formation of the $\text{Nd}_2\text{Fe}_{14}\text{B}$ phase, which can be confirmed in this work (figure 26 C). However the annealing process created another phase within the matrix of the material. These regions were identified by EDS analysis (figure 33) and contained 11at% Nd and 88at% Fe. This ratio suggests the formation of a $\text{Nd}_2\text{Fe}_{17}$ phase. This soft magnetic phase which will reduce the magnetic material's coercivity. The growth of this phase also means there will be a reduction in the $\text{Nd}_2\text{Fe}_{14}\text{B}$ phase as with the formation of αFe . Therefore this material should have more $\text{Nd}_2\text{Fe}_{14}\text{B}$ phase than the arc melted material (sample B) however less than the sintered magnet (sample A).

Around the edges of the annealed sample an oxide layer had formed (figure 28). This layer was visible by eye as a blackened layer surrounding the sample. The effect of oxygen on HDDR processing has been previously documented. If the sample is oxidised it can block hydrogen from entering the material. Skulj et al⁶¹ identified the oxide layer at these temperatures to contain Nd_2O_3 and Fe_2O_3 . Therefore the blackened oxide layer was manually ground off the sample prior to HDDR processing.

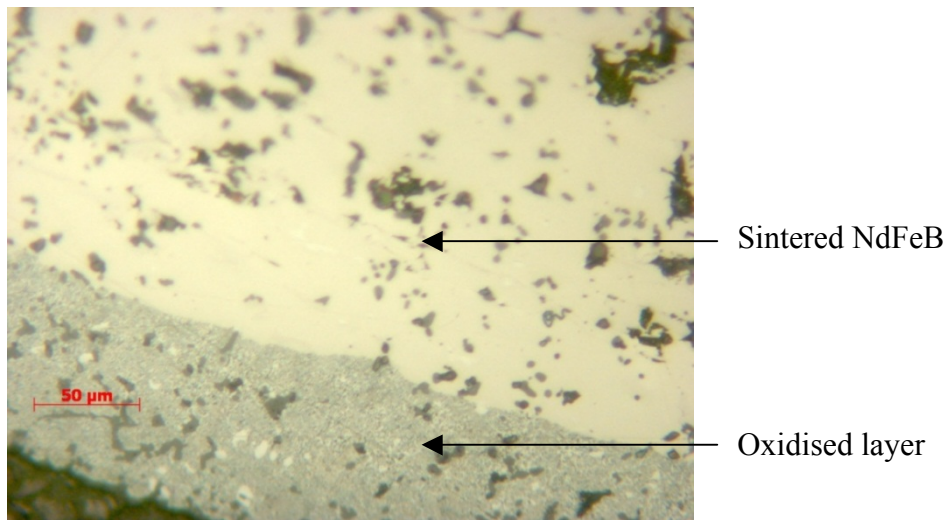
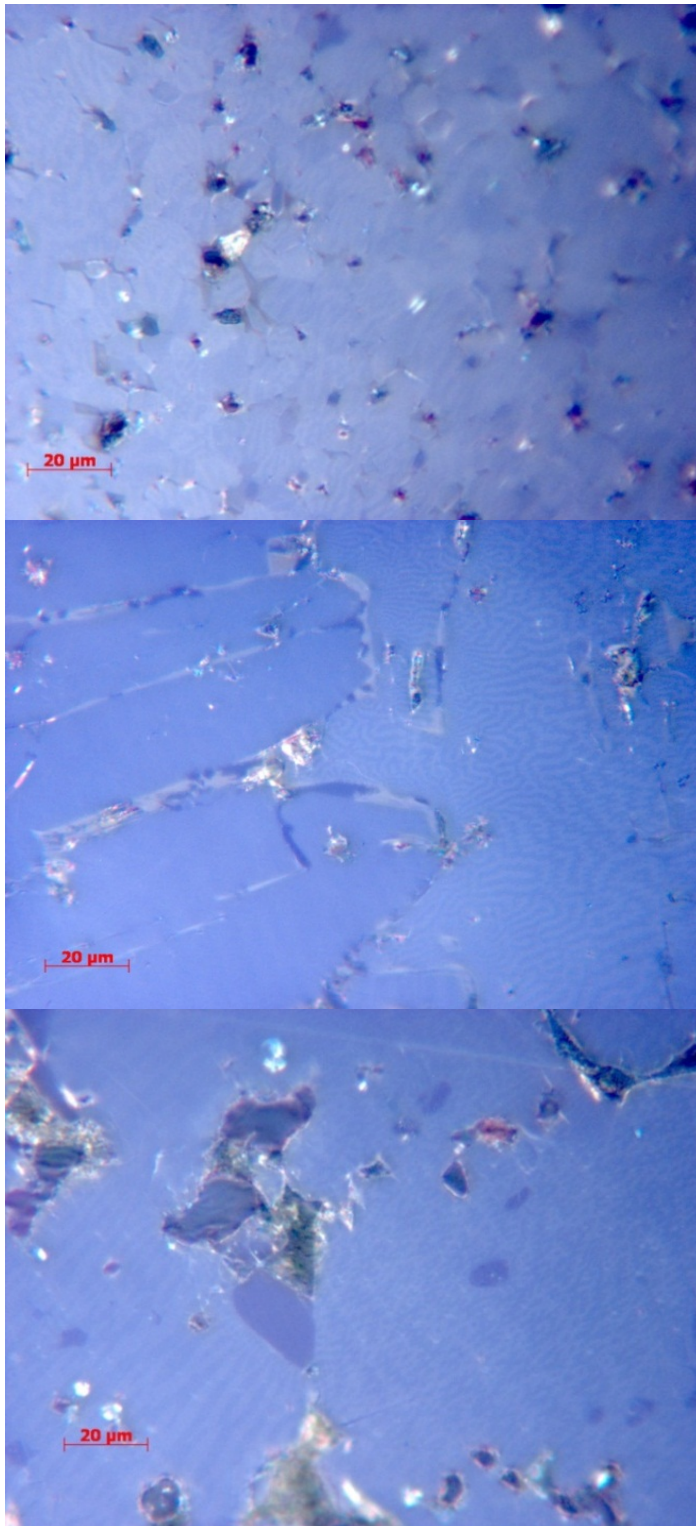


Figure 28: Optical microscope image of annealed material. Showing the blackened oxidized phase (bottom) and normal bulk material (top).



A)

Sintered starting magnet

B)

Arc melted material

C)

Annealed material

Figure 29: Optical microscope using Kerr imaging technique used to show the difference in grain size between A) Sintered starting magnet ($\text{Nd}_{13}\text{Fe}_{78}\text{Al}_{0.7}\text{Dy}_{0.8}\text{B}_{6.3}$) B) Arc melted material and C) Arc melted then annealed material.

Optical microscopy using a polarised lens was used to obtain Kerr effect images. These images were used to help quantify the size of the grains present at different heat treatments. For material A (sintered magnet) the grain size can was approximately 10-20 μm which is typical of that of commercially produced sintered magnets. The Kerr effect image also shows good alignment of the domains indicating good c-axis alignment.

The increase in grain size of the arc-melted material (B) is visible in the Kerr effect images in figure 29B. The grain size of the cast alloy is seen to be between 100-300 μm , considerably larger than the sintered magnet. The Kerr effect image also shows noticeable domain contrast between different grains. This suggests that during solidification from the liquid grains become aligned at random orientations.

From figure 26C it was shown that the process of annealing led to the removal of large areas of free iron within the material. However the free iron was not visible using Kerr effect microscopy. Figure 29C shows that the grain size of the annealed material is still much larger than that of the sintered magnet at approximately 200-400 μm . The annealed material contains large areas of Nd-rich pooled at grain boundary interfaces (figure 26C). Domain contrast between the grains is also still noticeable in the annealed material, similar to that of the arc-melted sample B. This suggests that the material is isotropic.

4.1.2 Altering Microstructure- Disproportionation curves.

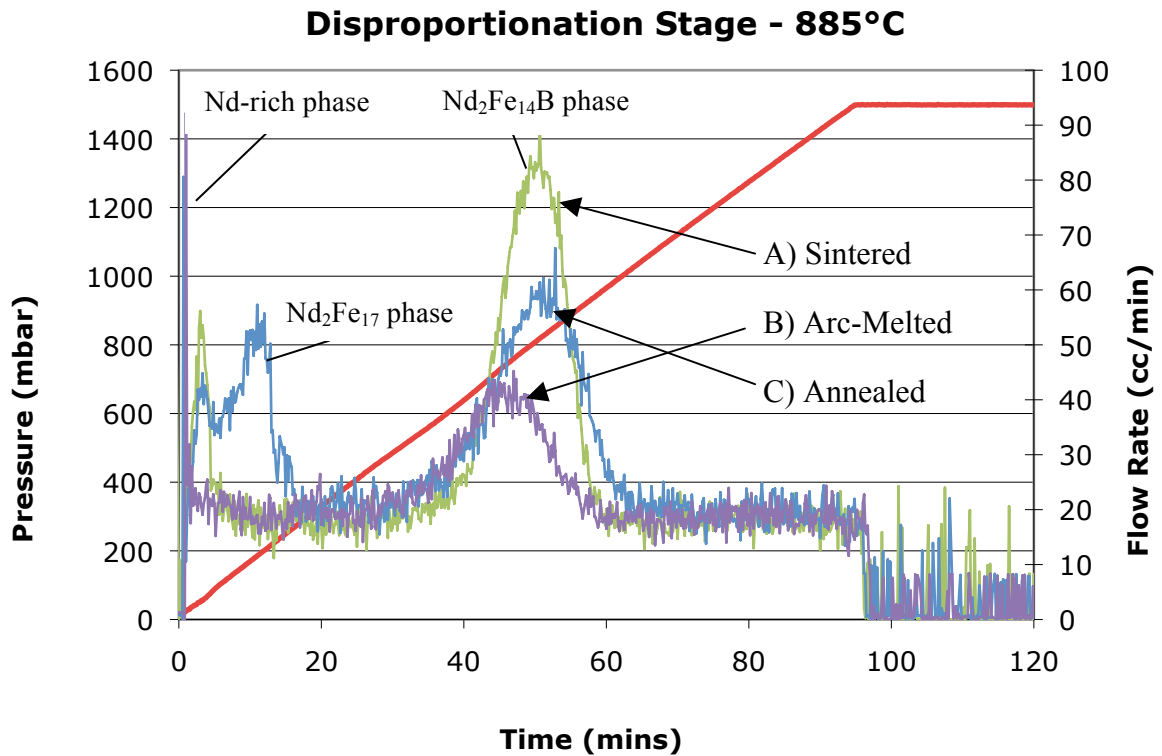


Figure 30 Disproportionation Curves obtained by altering $Nd_{13}Fe_{78}Al_{0.7}Dy_{0.8}B_{6.3}$ magnets Processed at $885^{\circ}C$ -1500mbar H_2 . Showing A) Sintered magnet microstructure, B) Arc melted microstructure and C) Annealed microstructure.

Sintered Magnet HDDR Disproportionation Curve

This disproportionation trace for the sintered magnet shown in figure 30A demonstrated a small Nd-rich peak at low pressures (left side) and a large $Nd_2Fe_{14}B$ phase peak (centre). The pressure of hydrogen at which disproportionation of the $Nd_2Fe_{14}B$ phase occurs is at approximately 700mbar, which is in agreement with previous work carried out by Sheridan et al⁵⁷ (figure 25). The area under the hydrogen curves can be used to estimate the proportion of the respective phases present. A small Nd-rich peak and $Nd_2Fe_{14}B$ phase peak indicates this material contained a larger quantity of matrix material than Nd-rich grain boundary phase.

Arc- Melted Magnet HDDR Disproportionation Curve

The disproportionation trace for the arc melted sintered magnet is shown in figure 30B. The material demonstrated an initial large sharp peak indicating a rapid hydrogenation of the Nd-rich phase. This peak had a higher intensity than that of any other material. The presence of free iron within this material would be expected to liberate more Nd to form the Nd-rich phase, due to the decrease in size of the $\text{Nd}_2\text{Fe}_{14}\text{B}$ phase. The pooling of large areas of Nd-rich will cause a rapid hydriding as shown by the sharp peak on the curve (figure 30B)

A broad peak is observed for the disproportionation of the $\text{Nd}_2\text{Fe}_{14}\text{B}$ phase indicating a slower absorption of hydrogen into the material due to the larger grain size. This could be due to the increased time hydrogen takes to penetrate from the grain boundaries into the centre of the matrix material. However the decrease in intensity of the peak indicates there is a reduced volume of $\text{Nd}_2\text{Fe}_{14}\text{B}$. This again might be due to an increase in free iron shown in figure 27. The disproportionation reaction for the $\text{Nd}_2\text{Fe}_{14}\text{B}$ initiates at a lower H pressure than that of the sintered magnet i.e. curve shifted to the left. This could be due to a change in the oxygen content of the materials during melting. The magnetic properties and microstructural analysis is shown in sections 4.1.3 and 4.1.4 respectively

Arc Melted-Annealed HDDR Disproportionation Curve

The HDDR disproportionation curve, which is shown in figure 30C, is of the arc melted then annealed material. Three distinct peaks were observed for this material. Initially a sharp peak was observed which is assumed to be the Nd-rich phase hydriding. The second peak would indicate the presence of a different phase within the material, compared to that of the sintered and arc melted materials, which reacts with hydrogen. From a review of the literature a common phase within the NdFeB system that is known to disproportionate is $\text{Nd}_2\text{Fe}_{17}$, which

was identified during electron microscopy studies on HDDR powders⁶². The presence of this soft magnetic phase can be detrimental to magnetic properties of a material. The third peak is that of the $\text{Nd}_2\text{Fe}_{14}\text{B}$ phase undergoing disproportionation. The broader peak indicates a slower disproportionation similar to that of the arc melted material. This could again be due to the large grain size when compared to the sintered magnet as seen in figure 26. Also the intensity of the peak is less than the sintered magnet, which suggests there is less $\text{Nd}_2\text{Fe}_{14}\text{B}$ phase present. This could be attributed to the formations of $\text{Nd}_2\text{Fe}_{17}$. The disproportionation peak however is larger than that for the arc melted material, which indicates that more of the matrix $\text{Nd}_2\text{Fe}_{14}\text{B}$ material is present in this sample. Further microstructural and magnetic property analysis for this material can be found in section 4.1.3 and 4.1.4 respectively.

4.1.3 Microstructural analysis of HDDR material

Each of the HDDR processed powders were mounted in conducting bakelite and examined using backscattered scanning electron microscopy equipped with EDS analysis.

A) Sintered magnet HDDR processed

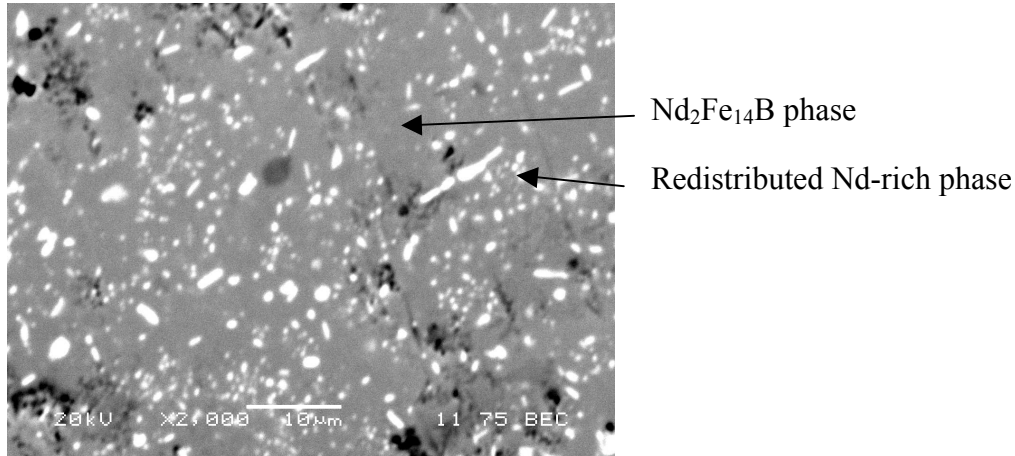


Figure 31: Backscattered SEM image of sintered magnet post HDDR processing showing fine re-distribution of Nd-rich and $\text{Nd}_2\text{Fe}_{14}\text{B}$ matrix phase.

Backscattered scanning electron microscopy of the sintered magnet shown in figure 31 indicates successful HDDR processing of the material. The image depicts a refined grain structure and re-distribution of the Nd-rich phase throughout the material, compared to the larger triple points observed in the starting sintered material. The re-distribution of the Nd-rich phase from the grain boundary area can lead to the development of pores within the powder. However the above image shows a powder, which has finely redistributed Nd throughout the material with no pores present. The magnetic properties for this material can be observed in section 4.1.4

B) Arc melted HDDR processed

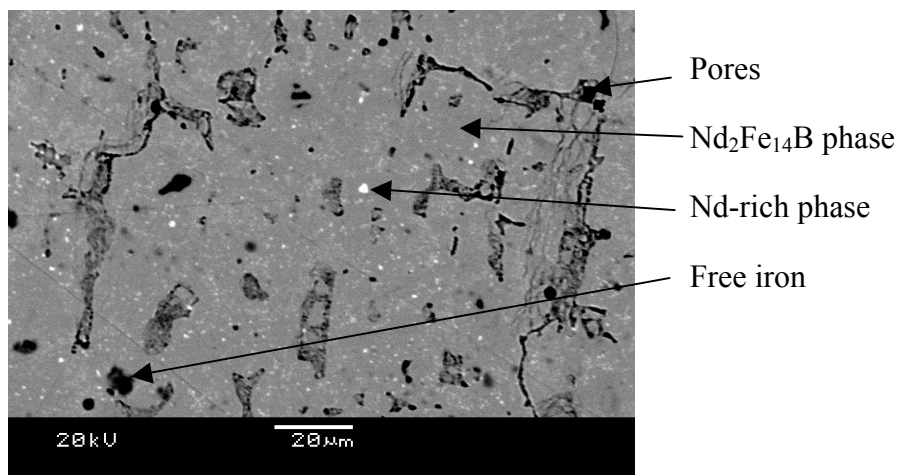
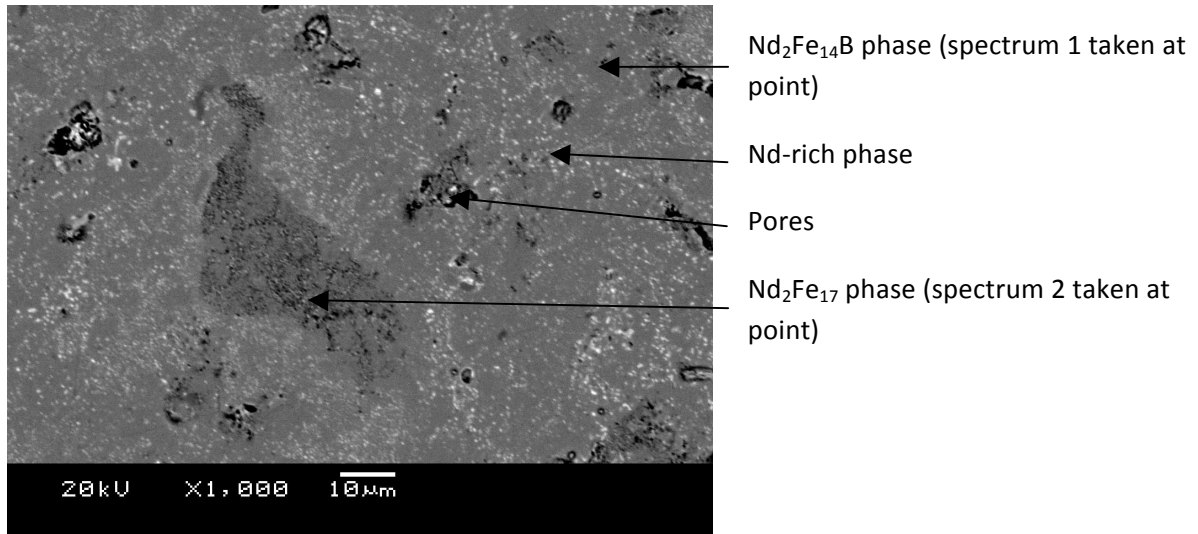


Figure 32: Backscattered SEM image of Sintered-Arc melted post- HDDR processed powder showing $\text{Nd}_2\text{Fe}_{14}\text{B}$ matrix phase, Nd-rich phase, pores and free iron.

The HDDR processed arc melted magnet powder is shown in figure 32. Figure 32 shows successful redistribution of the Nd-rich phase throughout the material, creating the desired fine ‘mottled’ effect. Pores are now present in the material; this is assumed to be due to the Nd-rich phase redistributing leaving large areas vacant. The Nd has moved into the $\text{Nd}_2\text{Fe}_{14}\text{B}$ phase which is observed as fine small white specks throughout the powder. However detrimental large areas of free iron remain within the material. The redistribution of the Nd-rich phase within the material would indicate that a finer grain structure has been developed.

C) Sintered Arc melted Annealed HDDR processed



EDS Spectrum 1:

Peak possibly omitted : 0.267 keV

Element	Weight%	Atomic%
Fe K	70.56	86.09
Nd L	29.44	13.91
Totals	100	

EDS Spectrum 2 :

Peaks possibly omitted : 0.265, 1.489 keV

Element	Weight%	Atomic%
Fe K	75.36	88.76
Nd L	24.64	11.24
Totals	100	

Figure 33: Backscattered SEM image with EDS analysis of sintered- arc melted- annealed HDDR powder. Showing Nd₂Fe₁₇ phase, Nd₂Fe₁₄B phase, redistributed Nd-rich into matrix phase and pores left from Nd-rich redistribution.

Microscopy of the HDDR processed arc melted then annealed powder is shown in figure 33. This exhibited a fine redistribution of the Nd-rich phase throughout the material. It also has some pores present as a result of the redistribution of the Nd similar to the arc melted material. However the annealed material disproportionation curve showed an extra peak compared to the other two materials. This peak occurred at approximately 200mbar, between the Nd-rich hydriding and the Nd₂Fe₁₄B disproportionating SEM/EDS analysis of the starting material showed that an Nd₂Fe₁₇ phase is likely to be present, which has been identified by a previous study⁶². After HDDR processing the Nd₂Fe₁₇ phase was shown to demonstrate a fine

microstructure indicating that this phase had disproportionated in line with the peak observed in figure 30.

4.1.4 Altering Microstructure- VSM Traces

Post HDDR processing the magnetic properties of the different materials were determined using a vibrating sample magnetometer. The results in the easy and hard directions are shown in figures 34 and 35.

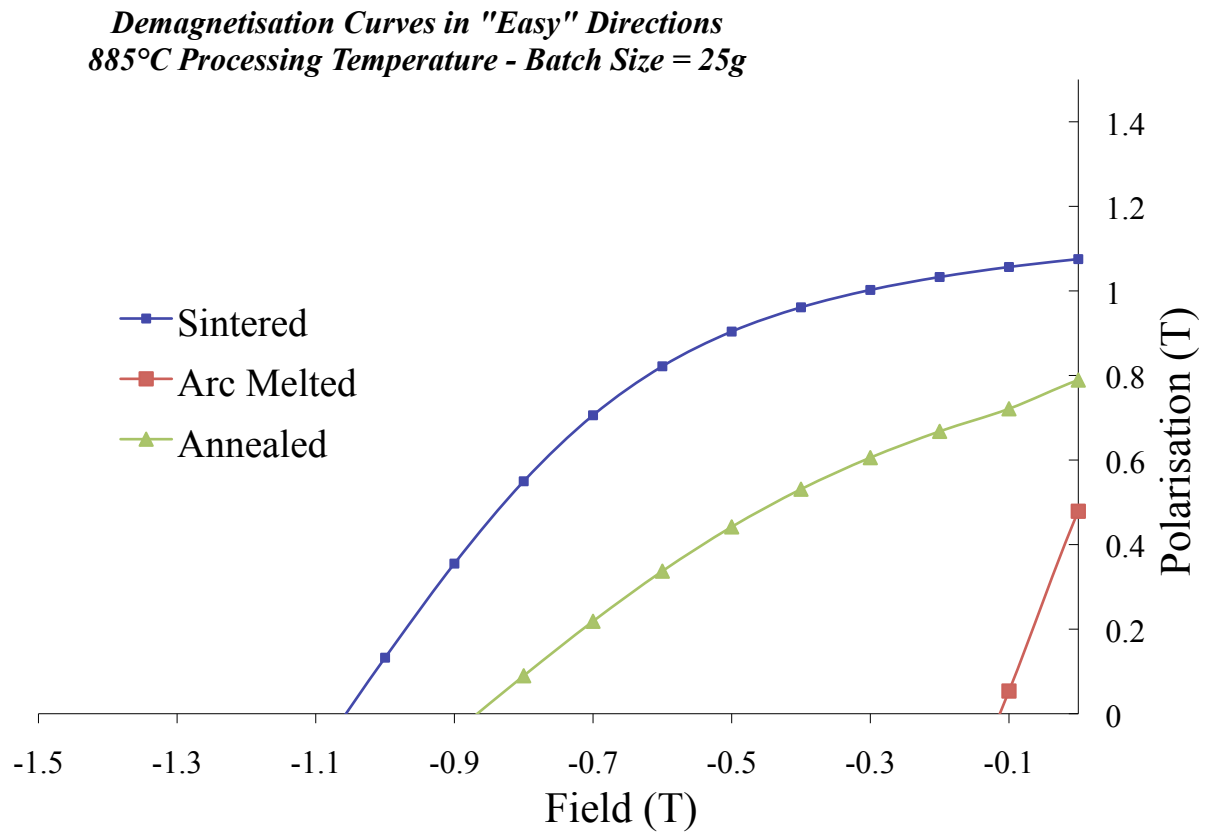


Figure 34: VSM curve in “Easy” direction, obtained from 20mg of a 25g HDDR powder batch.

***Demagnetisation Curves in "Hard" Directions
885°C Processing Temperature - Batch Size = 25g***

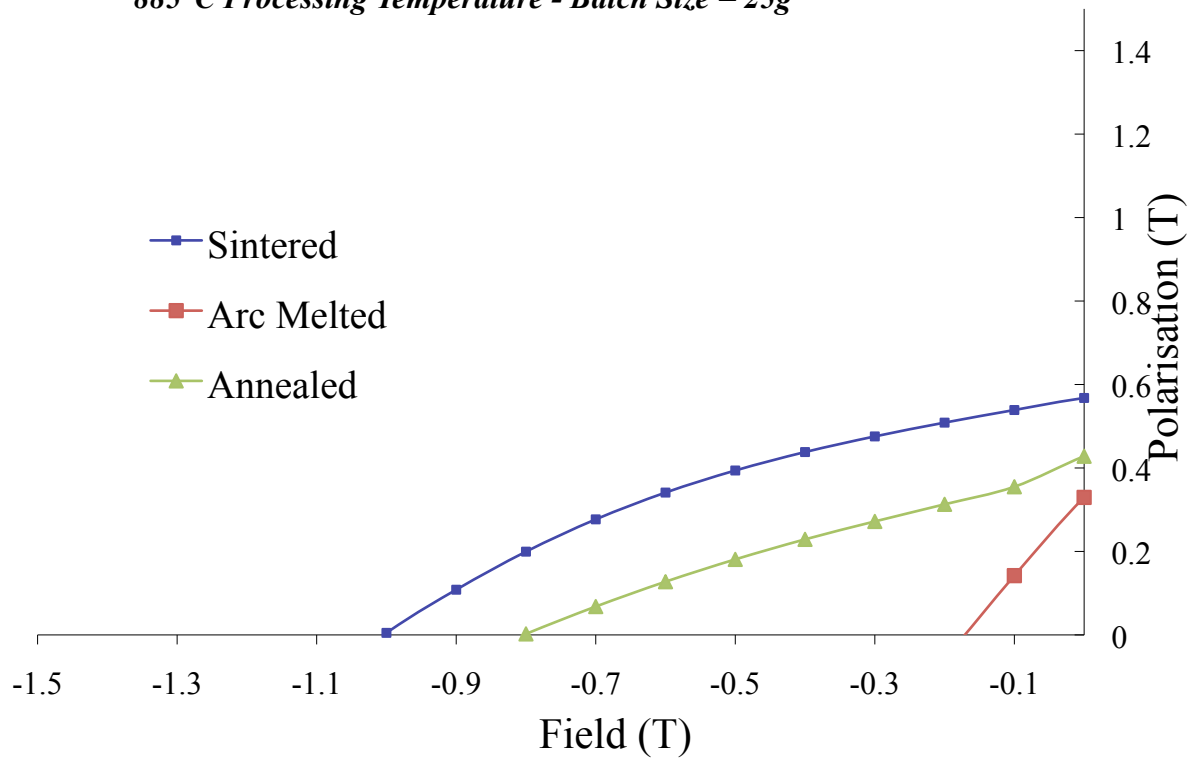


Figure 35: VSM curve in “Hard” direction, obtained from 20mg of a 25g HDDR powder batch.

The initial magnetic properties of the sintered starting magnet are:

Remanence: 1.36T Coercivity: 1.07T Energy Product 340kJ/m³

Sintered magnet HDDR powder:

The sintered magnet HDDR powder has the highest magnetic properties in terms of both remanence and coercivity when compared to the arc melted and annealed samples in both the easy and hard directions (figures 34 and 35). The magnetic properties are in agreement with Sheridans⁵⁷ reported results achieving an approximate remanence of 1.1T and a coercivity of 1.05T in the easy direction. A high degree of anisotropy exists in this material; as shown by high remanance in the easy direction. As discussed in section 2.3.2ii the anisotropy which is developed during HDDR processing is strongly dependant on the hydrogen pressure and

processing conditions during disproportionation^{28,29,30}. It is therefore apparent that for the sintered material the rate at which the disproportionation reaction occurred for the sintered magnet was slow enough to develop anisotropy within the HDDR powder.

Arc Melted HDDR powder:

The arc melted HDDR powder has both a low remanence and coercivity. This can be explained by the significant amounts of free iron present within the material as observed in figure 27. The presence of this soft magnetic phase acts as an initiation point for the growth of reverse domains, leading to the demagnetisation of the sample at lower fields. During the arc melting process any alignment that would have existed in the starting sintered material would have been lost creating an isotropic cast button. However the arc melted HDDR powder exhibited a degree of anisotropy. This can exist as during HDDR processing the large isotropic grains are refined into smaller ones, which retain the c-axis alignment of the original grain, as described in section 2.3.2ii.

Altering the grain size of the material is important, as it has been hypothesised that the HDDR process could be more effective on larger grained material. This is due to the way in which anisotropy is developed during HDDR processing. If the grain size of the material is increased it would be expected that during disproportionation many fine grains would develop all sharing the same c-axis alignment as the original large grain, and thus the material would have a high degree of anisotropy. However this may only be the case if the material is finely milled to separate each of the large cast grains prior to HDDR processing. In the experiment, hand milling using a pestle and mortar was undertaken, before the material was HDDR processed. This crushing process may have separated some of the large grains from one another however some large grains may have remained together. Therefore the degree of anisotropy exhibited by the heat treated materials would be expected as some grains are free to align during VSM testing where as others are still clumped together at random orientation.

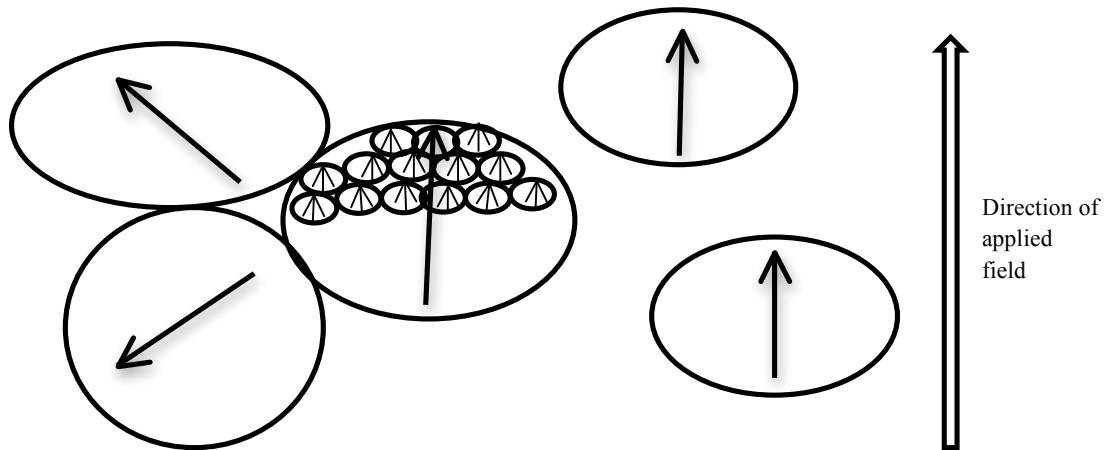


Figure 36: Schematic diagram showing how large grains can have high anisotropy if separated (RIGHT) however can be isotropic if individual grains are still joined (LEFT).

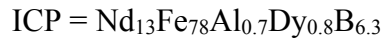
Annealed HDDR powder:

From backscattered SEM analysis (figure 33) it can be observed that the annealing process has removed large quantities of the free iron present in the arc melted material. As a result the magnetic properties have been greatly improved. The remanence and coercivity of the material in the easy direction is approximately 0.8T and 0.85T respectively. However the magnetic properties of the annealed material are not as high as that of the sintered magnet. This may be due to the inclusion of the $\text{Nd}_2\text{Fe}_{17}$ soft magnetic phase that appears to have formed during annealing (figure 33). Similar to the presence of iron within the arc melted material, a soft magnetic phase can act as an initiation point for the growth of reverse domains leading to a lower coercivity. Once again a degree of anisotropy existed within this material.

4.2 Comparing sintered magnets with the different compositions

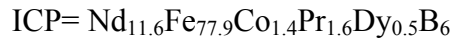
Two sintered magnets with different compositions were HDDR processed. The two materials selected were:

Sintered 'starting' magnet:



Remanence: 1.36T Coercivity: 1.07T

Sintered magnet produced by Philips:



Remanence: 0.83T Coercivity: 1.45T.

The objective of this section of the report was to investigate if it is possible to HDDR process different sintered magnets composition using the same set of processing conditions.

4.2.1 Comparison between Sintered Magnets- Disproportionation Curves

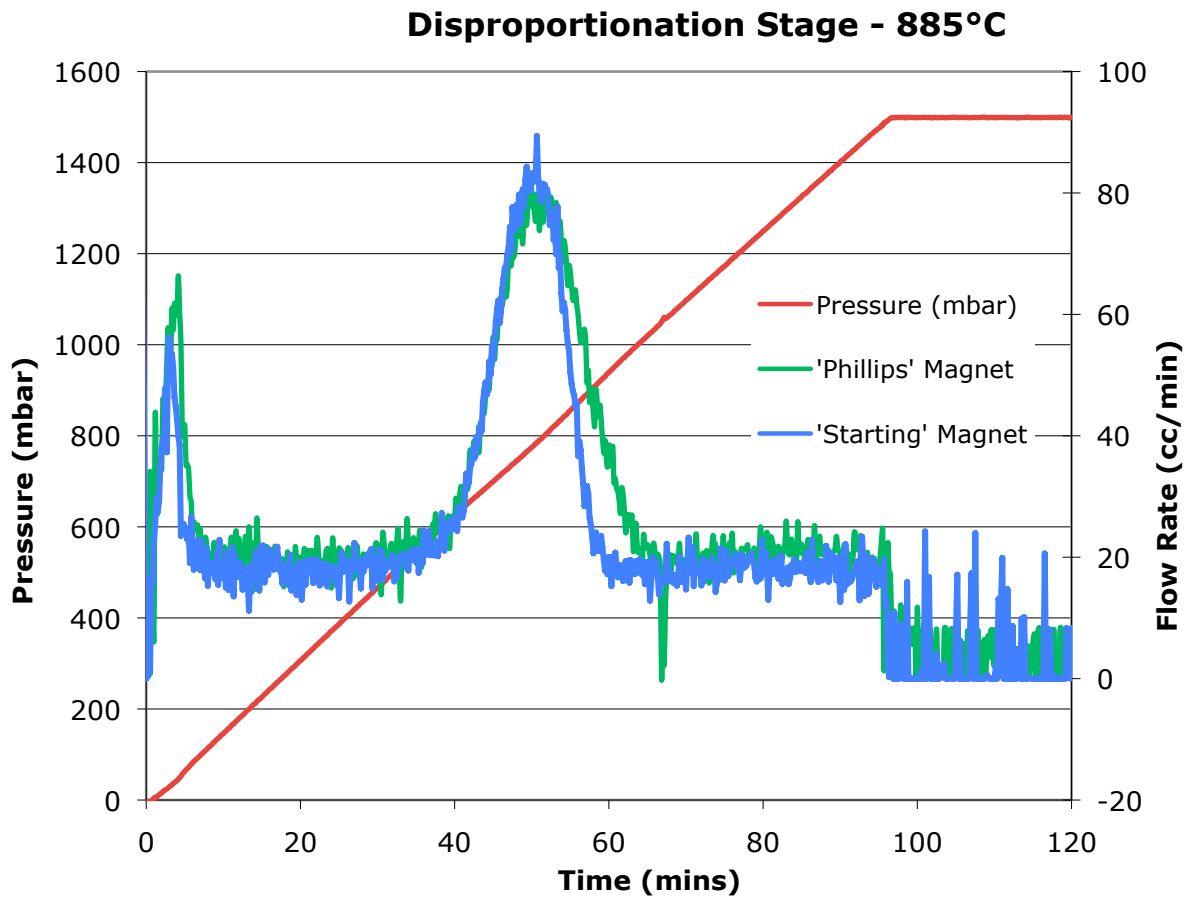


Figure 37: Disproportionation Curve showing comparison between two sintered magnets.

Processed at 885°C – 1500mbar H.

The 'Philips' magnet used in this experiment was previously used in a hard drive disk as part of the voice coil motor assembly. The protective nickel coating was ground and peeled off prior to HD and HDDR processing. The disproportionation curve, shown in figure 37, suggests that both materials underwent a very similar disproportionation stage. Both materials show a noticeable peak at low hydrogen pressures as the Nd-rich phase hydrides. Then a delay as the hydrogen pressure is increased until it reaches approximately 700mbar and the $\text{Nd}_2\text{Fe}_{14}\text{B}$ phase disproportionates. The initiation of disproportionation occurs at the same time, despite their differences in composition. The 'Philips' magnet has a peak of a similar height to that of the starting sintered magnet used in previous experiments. This indicates that they contain similar levels of the matrix $\text{Nd}_2\text{Fe}_{14}\text{B}$ phase. However the time taken until completion of the disproportionation stage appears to be approximately 10mins longer. This could be due to the inclusion of Co present in the Philips magnet. Co has been shown to slow the disproportionation reaction rate (section 2.4.1). From figure 37 it is difficult to distinguish any key differences between the ways these two materials processed.

4.2.2 Comparison between Sintered Magnets – VSM results.

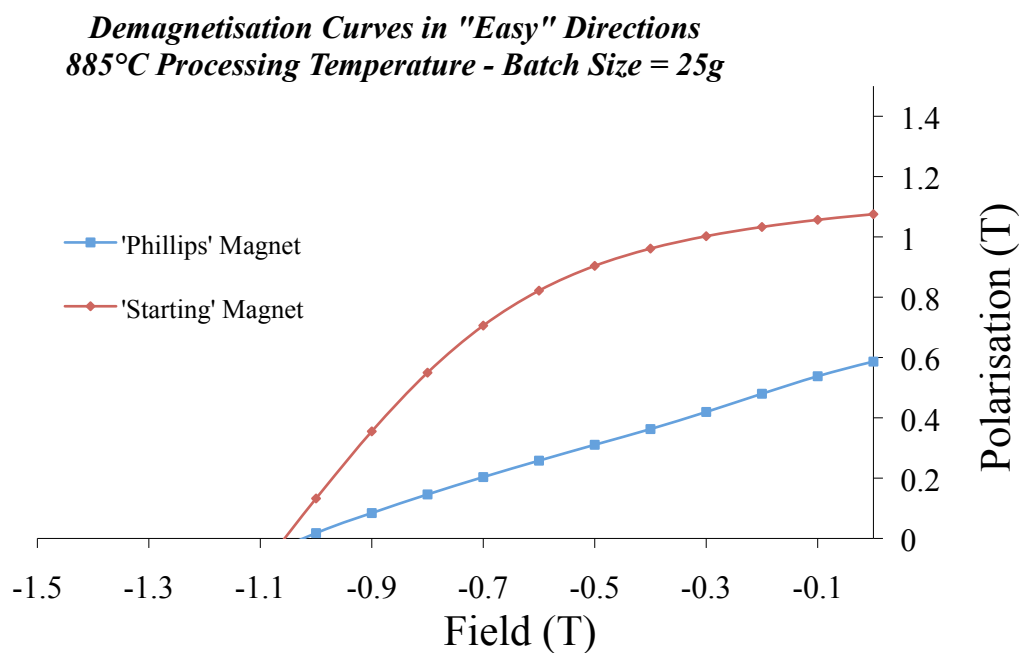


Figure 38: VSM trace showing 'Easy' direction of magnetization for 'starting' HDDR powder and 'Phillips' HDDR powder.

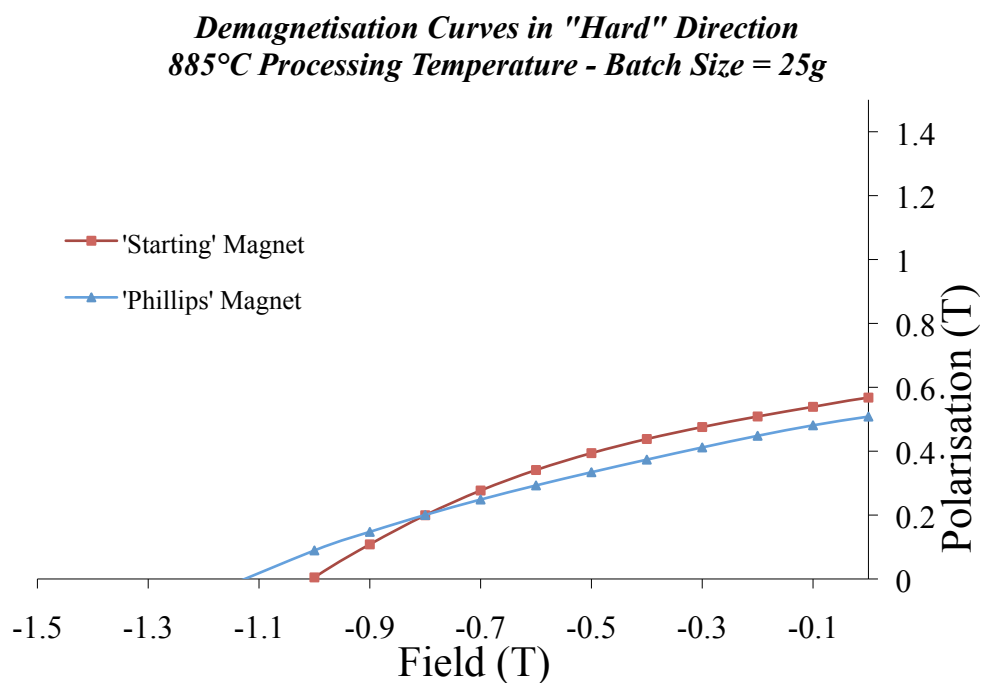


Figure 39: VSM trace showing 'Hard' direction of magnetization for 'starting' HDDR powder and 'Phillips' HDDR powder.

Despite the fact that the disproportionation curves for the Philips magnet and the starting sintered magnet look very similar, the magnetic properties vary significantly. A very weak anisotropy was exhibited by the 'Philips' HDDR powder. This is shown on the VSM trace by little difference in the magnetic properties in both the 'Easy' and 'Hard' directions. When Co is added to NdFeB alloys this has been shown to increase the disproportionation pressure and increase the observed anisotropy (section 2.4.1). However this is not the case in this study. Later work carried out by Sheridan et al⁶⁰ has demonstrated that by decreasing the hydrogen pressure to 1200mbar, during HDDR processing, it is possible to develop significant anisotropy in the Philips HDDR powders. Therefore it can be assumed that under the HDDR conditions used in this study that the material over-processed. It is not clear as to why this is the case and further work is required in this area. It is clear that the processing conditions outlined in this study would not be suitable for processing a range of sintered scrap feeds if anisotropic material is required.

4.3. An investigation into HDDR processing of cast materials with varying Nd content

From section 4.2 it can be observed that it is possible to process sintered magnets via the HDDR route. However despite both materials appearing to process in similar ways the magnetic properties varied significantly. In this section of the project the aims are to investigate the effect of cast alloys with different Nd-ratios. These were then compared to the starting sintered magnet. The materials used in this section were:

A) Medium rare earth cast block-ICP= $\text{Nd}_{13}\text{Fe}_{78}\text{Al}_{0.4}\text{B}_{7.4}$

B) Higher rare earth cast block- ICP= $\text{Nd}_{15.6}\text{Fe}_{75}\text{Al}_{0.7}\text{B}_{8.2}$

C) Sintered magnet- ICP = $\text{Nd}_{13}\text{Fe}_{78}\text{Al}_{0.7}\text{Dy}_{0.8}\text{B}_{6.3}$

The above cast materials (A and B) were selected from the lab due to them sharing a similar composition and do not include many additional alloying elements. The Al ratio did vary slightly as shown from the ICP results. The addition of Al has been shown to affect the observed magnetic properties of the material and degree of anisotropy (section 2.4.3). However there is no evidence as to their effect on the HDDR process. The disproportionation curves for the materials are shown in figure 40.

4.3.1 Altering Nd Content- Disproportionation curves

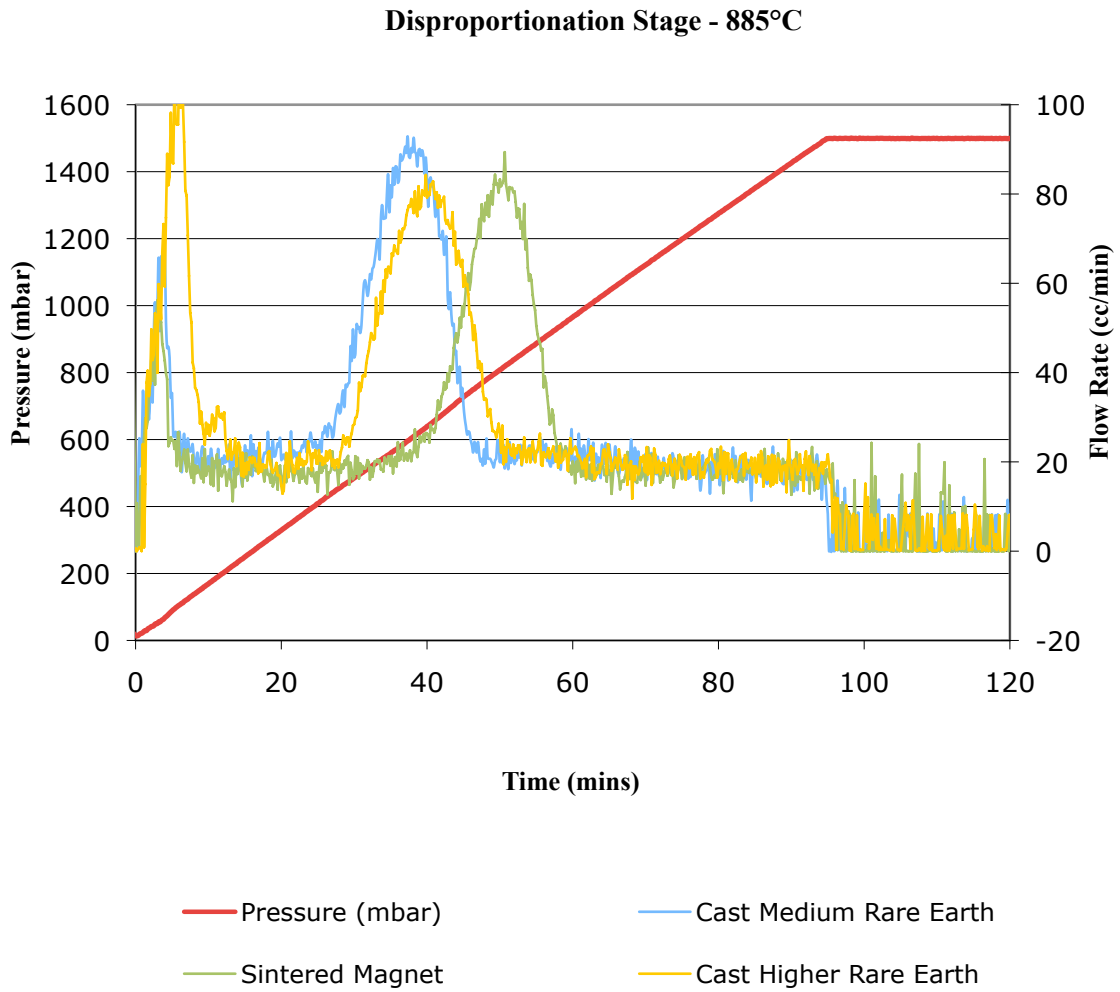


Figure 40: Disproportionation curve showing; Cast ($\text{Nd}_{13}\text{Fe}_{78}\text{Al}_{0.4}\text{B}_{7.4}$) ‘Medium’ Rare earth magnet, Cast ($\text{Nd}_{15.6}\text{Fe}_{75}\text{Al}_{0.7}\text{B}_{8.2}$) ‘Higher’ Rare earth magnet and Starting ($\text{Nd}_{13}\text{Fe}_{78}\text{Al}_{0.7}\text{Dy}_{0.8}\text{B}_{6.3}$) Sintered Magnet. Processing conditions: 885°C 1500mbar H pressure.

The disproportionation curve shown in figure; shows that each material exhibited an Nd-rich hydriding peak (left) and a disproportionation peak (centre). However the pressures and intensities of each of these peaks varied between each sample.

The ‘Medium’ Nd content cast material had a smaller Nd-rich peak and a larger $\text{Nd}_2\text{Fe}_{14}\text{B}$ disproportionation peak than the ‘Higher’ Nd content cast material. The initial differences in

the Nd-rich hydriding peak would be expected as the 'Higher' Nd content material would have an increased volume of Nd-rich grain boundary area. It would therefore be expected that the disproportionation peak for the high rare earth content material would be smaller as it contains less $\text{Nd}_2\text{Fe}_{14}\text{B}$ phase. Book et al⁶³ demonstrated this previously using the c-HDDR process on cast NdFeB material. This study examined two materials $\text{Nd}_{13}\text{Fe}_{80}\text{B}_{6.5}$ and $\text{Nd}_{16}\text{Fe}_{76}\text{B}_8$ which have similar compositions to those used in the current study. However in Books⁶³ study both cast materials initiated disproportionation at the same temperature when heated under 1bar of hydrogen. In this work however the disproportionation peak for the 'higher' rare earth material is shifted to the right. It is not clear why this occurs and there is no description of this in the literature. It may have been expected that the higher rare earth content material would lead to a faster processing time due to an expected rapid entry of hydrogen into the material along Nd-rich grain boundary regions. Another possible explanation is the small difference in Al ratio could have had an effect on the HDDR processing. However as mentioned this is unreported.

The disproportionation curve shown in figure 40 also shows a clear difference between the sintered magnet and cast NdFeB materials. This is expected as these materials have several key differences, which would affect the disproportionation. It can be observed that the $\text{Nd}_2\text{Fe}_{14}\text{B}$ phase in the cast materials underwent disproportionation at much lower hydrogen pressures compared to the sintered magnet and both completed sooner.

It may have been expected that the large grains in the cast material would take a longer time to process (as discussed in section 4.1). However it would appear that other variables are having a bigger impact on the disproportionation start and end points in this study.

The oxygen content of a sintered magnet is usually between 2000-4000ppm, whereas for cast material would be expected to be 200-300ppm. The effect of oxygen has been shown to affect the thermodynamics and kinetics of the disproportionation reaction (section 2.5). It is expected that the increase of oxygen content will increase the pressure at which disproportionation will initiate. This would account for the increase in disproportionation initiation pressure observed here.

The final difference between the sintered magnet and cast material is the addition of Dy. This addition was described in section 2.4.2. It is difficult to find sintered scrap sources which do not contain the addition of Dy. Similar to increasing the oxygen content of the material additions of Dy will increase the hydrogen pressure required to start disproportionation. The combined effect of increased oxygen content and the addition of Dy would explain the differences observed between the sintered magnet and cast NdFeB disproportionation curves.

4.3.2 Altering Nd content- VSM results.

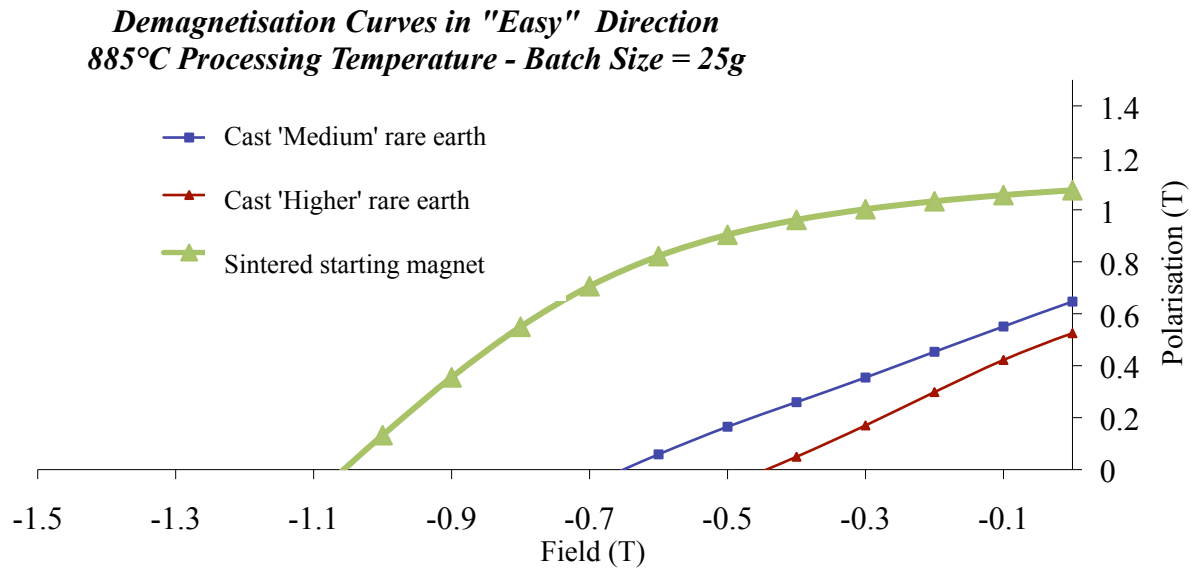


Figure 41: VSM trace showing “Easy” direction of magnetization of sintered ‘starting’ magnet, cast ‘medium’ rare earth and cast ‘higher’ rare earth.

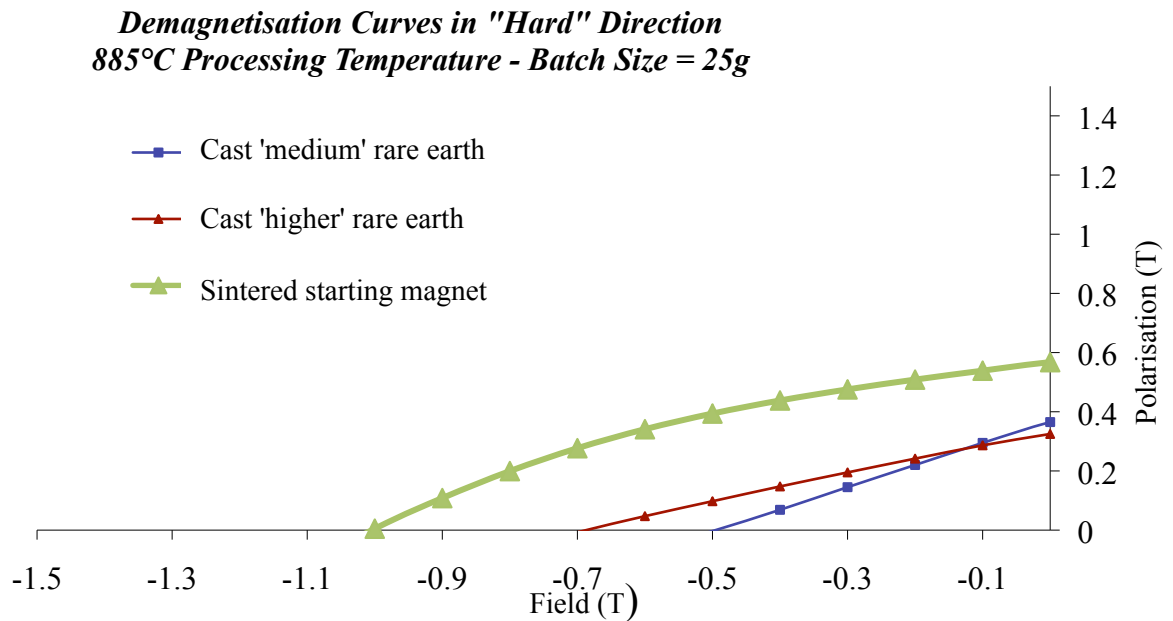


Figure 42: VSM trace showing “Hard” direction of magnetisation of sintered ‘starting’ magnet, cast ‘medium’ rare earth and cast ‘higher’ rare earth.

The VSM results, in figures 41 and 42, show that both cast materials have fairly poor magnetic properties. A low remanance and coercivity is exhibited in both easy and hard directions. The ‘Low’ rare earth HDDR powder had better magnetic properties in the ‘Easy’ direction than the ‘Medium’ rare earth HDDR powder. However an interesting observation is the development of some anisotropy in the higher Nd content cast sample. This has been discussed in a paper by Morimoto et al⁶⁴ who carried out a study into coercivity enhancement in anisotropic Dy-free NdFeB cast materials. Morimoto observed that the coercivity and alignment of HDDR powders increased as the Nd content was increased, and is further improved by a slow desorption with higher Nd content material. The study concluded that highly coercive and aligned powders could be due to the redistribution of Nd-rich grain boundary phase, which continuously surrounds the Nd₂Fe₁₄B grains.

The overall poor magnetic properties observed for the cast materials could be due to over processing of the powders. As shown in figure 40 both cast materials had finished disproportionation after approximately 50 minutes. However the HDDR process continued for an additional 70 minutes. Over processing of conventional HDDR powders is known to exist and it is expected that a similar effect would happen in dynamic HDDR processing. A schematic of this process is shown in figure 43.

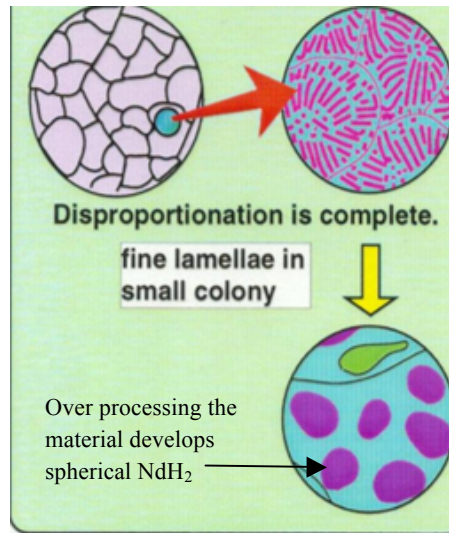


Figure 43: Schematic diagram of over-processing of NdFeB material when processed by c-HDDR route.

During over processing (figure 43) it can be observed that continued heating leads to the development of spherical NdH₂, which is embedded in the Fe. Larger NdH₂ clumps leads to the development of a coarse grain structure on recombination and loss of anisotropy. If this theory is applied to the materials investigated in this study then it is possible that the HDDR processing conditions used lead to over processing of the cast materials and a reduction in the observed magnetic properties.

Conclusion

5.1 The effect of microstructure on HDDR processing

Commercial grade sintered magnets were chosen for this project with compositions which match those found in the most common form of scrap i.e. electronic devices. These magnets have relatively low Nd and Dy contents compared to magnets used in high-energy motors. It was however not possible to gain access to these compositions as a cast commercial alloy, therefore the sintered magnets were heat treated to change the microstructure of the material. The heat treatments selected altered the observed grain size of the sintered magnet. However it was apparent that the effect of altering the microstructure during melting and subsequent heat treatments was overshadowed by other variables. Free iron was formed during arc melting and then $\text{Nd}_2\text{Fe}_{17}$ was formed during annealing. Oxidation of the sample during annealing is the most likely cause for the formation of $\text{Nd}_2\text{Fe}_{17}$. Another cause could also be due to the sublimation of Nd on heat treatment. If the annealing process was carried out at a higher vacuum then oxidation of the sample could be prevented or minimised.

5.2 Comparison between sintered magnets with different compositions

The Philips sintered magnet ($\text{Nd}_{13}\text{Fe}_{77.8}\text{Al}_{0.7}\text{Dy}_{0.6}\text{B}_{6.4}$) was chosen for the HDDR studies as it originates from a voice coil motor assembly in HDDs. HDDs are the most abundant scrap stock available for recycling today. The HDDR processing curves (disproportionation shown in 4.2.1 and recombination in appendix) for the Philips magnet and starting Chinese sintered magnet ($\text{Nd}_{13}\text{Fe}_{78}\text{Al}_{0.7}\text{Dy}_{0.8}\text{B}_{6.3}$) was very similar HDDR. However the end magnet anisotropy observed for the Philips magnet was surprisingly poor. Later work has demonstrated by Sheridan et al⁶⁰ has shown that processing at a lower hydrogen pressure (1200mbar) has led to the development of anisotropy. This would imply that over processing is the primary reason

for the loss in properties. It is however unclear why the starting sintered magnet didn't demonstrate a similar fall in anisotropy given the similarities in the disproportionation and recombination curves. It is evident that even slight variations in scrap material composition can have a big effect on how well the HDDR process will work. Further work is required to investigate the HDDR processing of a wider range of compositions

5.3 Altering Nd content in cast alloys

Cast alloys with varying Nd ratios were used to investigate the effect of altering Nd content on HDDR processing. The higher Nd content cast material demonstrated a higher hydrogen peak during the Nd-rich hydriding ($>1600\text{mbar}$) and a smaller peak ($\sim 1350\text{mbar}$) for the disproportionation curve, compared to the lower rare earth content material that peaked at approximately 1500mbar . This would be expected as mentioned previously in section 4.3.1. However it was not clear why the higher rare earth material underwent disproportionation at a higher hydrogen pressure therefore the results seen in this study may be due to sample variation and further work will be required to understand this.

It was evident that the cast materials were disproportionating at much lower pressures than the sintered magnets and therefore it is unlikely that it will be possible to process cast and sintered magnets under the HDDR process conditions shown here. Over processing is very likely to have occurred to the cast materials due to excess time spent at a high temperature and hydrogen pressure. This over processing drastically reduced the magnetic properties of the powder leading to poor anisotropy and magnetic properties as shown in section 4.3.2. Therefore when considering HDDR recycling it would be important to separate cast and sintered materials due to differences in both grain size and oxygen content.

5.4 Summary

In conclusion it is evident that the HDDR conditions used in this work are only appropriate for specific sintered magnet compositions. It has been shown that if the composition varies significantly then the magnetic properties achieved are extremely poor. One potential scrap application which has magnets with a narrow compositional range is HDD magnets.

If the HDDR route were to be applied outside of the HDD application, for example to magnets in drive motors of electric vehicles then the composition would be significantly different to the HDDs (higher Dy content >8% of rare earth content). This variation is likely to dictate the HDDR processing conditions if an anisotropic powder is to be developed.

Future Work

In order to better understand the effect of microstructure on HDDR process better control of the starting materials is required. A pilot scale strip casting facility is being built at the University of Birmingham, which will allow the group to produce its own specific alloy composition. If this technique was perfected it could be used as a starting material for HDDR processing. This would allow for removal of both α -Fe and $\text{Nd}_2\text{Fe}_{17}$.

Since experiments in this report were completed, further work has been carried out at the University of Birmingham on HDDR processing of the Philips magnet. The study has shown that HDDR processing the Philips magnet at lower hydrogen pressure (1200mbar) resulted in improved magnetic properties and an anisotropic powder being created⁶⁵. Further microstructural analysis, using high resolution SEM techniques, would be useful to examine the difference between the two Philips samples that were HDDR processed at different hydrogen pressures.

It is evident that a wider study is required taking into account a larger compositional range of magnets from a variety of applications. It is hoped that this will allow us to further understand and optimise the HDDR recycling process.

References

- [1] Hatch. G. (2012) *Recent dynamics in the global rare earths market* 22nd International workshop on rare earth permanent magnets and their applications p4
- [2] Hatch. G. (2010) *Geopolitics and the rare earth magnet supply chain*, UK Magnetism Society One Day Seminar.
- [3] Muniz-Casias, C. (2011) *Permanent magnet solutions in wind*. UK Magnets Society One Day Seminar
- [4] Allcock, R. (2010) *Rare earth materials – how scarce are they?* UK Magnetism Society One Day Seminar
- [5] Toyota Motor Corporation (2009) news release viewed on 27/03/13
<http://green.autoblog.com/2009/09/04/toyota-tops-2-million-hybrid-sales-worldwide/>
- [6] Ombach, G. (2010) *Development trends in area of small electric motors for automotive applications* UK Magnetic Society One Day Seminar
- [7] Junak, J. (2010) *Development trends in area of small electric motors for automotive applications* UK Magnetism Society One Day Seminar
- [8] Hill, J. (2010) *Wind turbines- the era of the permanent magnet generator* UK Magnetic Society One Day Seminar
- [9] Hitachi Recycling technologies (2010) viewed 27/03/13 <http://phys.org/news/2010-12-hitachi-recycling-technologies-rare-earth.html#jCp>
- [10] Walton, A. Yi, H. Rowson, H. Speight, J.D Harris, I.R. Williams. A.J (2012) *The Use of Hydrogen to Separate and Recycle NdFeB Magnets from Electronic Waste Processings* 22nd International workshop on RE permanent magnets and their applications
- [11] Kronmuller H, Durst K. D and Sagawa M (1988) *Analysis of the magnetic hardening mechanism in Re-FEB permanent magnets* J. Magnets and Magnetic materials 74(3) p291
- [12] Herbst J.F, Croat J.J, Pinkerton F.E and Yelon W.B (1984) *Relationships between crystal-structure and magnetic properties in Nd₂Fe₁₄B* Physics Review, B29 p4176
- [13] Matsuura Y., Hirosawa S., Yamamoto H., Fujimura S. and Sagawa M. (1985) *Magnetic properties of the Nd(Fe-1XCoX)₁₄B system* Journal of Applied Physics (46)3 p308-310
- [14] Sagawa M, Hirosawa S, Tokuhara K, Yamamoto K, Fujimura S, Tsubokawa Y, and Shimizu R. (1987) *Dependence of coercivity on the anisotropy field in the Nd₂Fe₁₄B type sintered magnets*. Journal of Applied Physics (61)
- [15] Braun H. F, Perizzone M and Yvon K; (1982) 7th International Conference on Solid Compounds and Transition Elements, Grenoble, II B2
- [16] Givord D. Moreau J. M and Tenaud P; (1985) Solid State Commun., 55 p303

- [17] Fidler J. (1987) IEEE Trans.Magn. Vol.23, No 5 p 2106
- [18] Hiraga K, Hirabayashi M, Sagawa M and Matsuura Y; Jap (1985) J. Appl.Phys., 24, No 6 p699
- [19] Niarchos D, Zouganelis G, Kostikas A and Simpoulous A; (1986) Solid Stat Commun., 59 p389
- [20] Durst K.D, and Kronmuller H; (1987) Journal of Magnetism and Magnetic Materials., 68 p63.
- [21] Sun A.Z. Shen W. Xu H, Wang J. Zhang Q. Zhai F and Volinsky A. (2012) *Nd₂Fe₁₇ nanograins effect on the coercivity of HDDR NdFeB magnets with low boron content*. Int J of Mineral, Metallurgy and Materials Vol 19. 3 p.236
- [22] Wang X.D, Wang X, Sun B.Y and Fang Y. (2007) *Fabrication of NdFeB magnetic powders by developed strip casting method* 8th Vacuum Metallurgy and Surface Engineering Conference p57-63
- [23] Harris I.R (1994) Concerted European Action on Magnets (EU Consortium)
- [24] Zakotnic M, Devlin E, Harris I.R, Williams A.J, Proceedings of 19th international workshop on rare earth permanent magnets and their applications.
- [25] Takeshita. T and Nakayama R. (1989) 10th Int. Workshop on RE Magnets and their Applications, Japan 551
- [26] McGuinness P. J, Devlin E, Harris I. R Rosendaal E and Ormerod J., (1989) *J. Of Material Science* 24 2541-2548
- [27] Gutfleisch O., Gebel B, Mattern N, (2000) *Texture in a ternary Nd_{16.2} Fe_{78.2} B_{5.6} powder using a modified HDDR process*. J. Magnetism and Magnetic Materials 210 L5-L9
- [28] Mishima C, Hamada N, Mitarai H. and Honkura Y. (2001) *Development of a Co free anisotropic bonded magnet produced from HDDR processed powder* IEEE Transactions on magnetics, Vol 37, No. 4
- [29] Kwon H. W, Yu J.H, (2009) *Effect of hydrogen pressure on disproportionation kinetics of Nd-Fe-B alloy* Journal of Alloys and Compounds (487) p138-141
- [30] ¹ Honkura Y, Mishima C, Hamada N, Drazic G and Gutfleisch O. (2005) *Texture memory effect of Nd-Fe-B during hydrogen treatment*. J. Magnetism and Magnetic Materials. 290-291. p1282-1285.
- [31] Guth K, Woodcock T.G, Schultz L, Gutfleisch O, (2011) *Comparison of local and global texture in HDDR processed NdFeB magnets* Acta Materialia 59 p2029-2034
- [32] Sugimoto S, Nakamura H, Kato K, Book D, Kagotani T, Okada M and Homma M (1999) *Effect of the disproportionation and recombination stages of the HDDR process on the*

inducement of anisotropy in NdFeB magnets. Journal of Alloys and Compounds 293-296 p862-867

[33] Takeshita T and Nakayama R, (1989) Proc. 10th Int. Workshop on Rare Earth Magnets and Their Applications, Kyoto, p. 551

[34] Ragg, O.M., Nagel H., Keegan G. And Harris, I.R (1996) *Recent Developments in the Study of HDDR Materials*. Proc. 14th Int. Workshop on Rare Earth Magnets and their Applications p.A8-A27

[35] Sagawa M, Fujimura S, Yamamoto H, Matasuura Y and Hiraga K. (1984) IEEE Trans Magn MAG-20, 1584

[36] Takeshita T and Nakayama, R (1991) Proc. 11th Int. Workshop on Rare Earth Magnets and their Applications, p. 49.

[37] Nakamura H., Suefuji R., Sugimoto S., Okada M and Homma M. (1994) Journal of Applied Physics, 76, p6828

[38] Kim, A.S. (1988) Journal of Applied Physics, pg 3519-3521

[39] Guth K, Woodcock T.G., Schultz L and Gutfleisch O., (2012) *Recycling of sintered NdFeB magnets by the d-HDDR route*. Proc. 22nd Int Workshop on Rare Earth Magnets and their Applications

[40] Rodewald W and Fernegel W. (1988) IEEE Trans, Magn. MAG-24,2, 1638

[41] Mizoguchi T, Sakai I, Niu H, Inomata K. (1986) *Nd-Fe-B-Co-Al Based Permanent-Magnets With Improved Magnetic-Properties And Temperature Characteristics*. IEEE Transactions on Magnetism. 22(5) p 919-921.

[42] Knoch K.G., Henig T. And Fidler J (1990) Journal of Magnetism and Magnetic Materials 83, 209-210

[43] Galego E, Takiishi H and Nunes de Faria Jr.R. (2007) *Magnetic properties of Pr-Fe-Co-B bonded HDDR magnets with alloying additions* Mat. Res. vol.10 no.3 São Carlos

[44] Shimoda T, Akioka K, Kobayashi O and Yamagami T. (1988) J of applied Physics 64 5290.

[45] Knoch K. G, Kianvash A. and Harris I. R. (1992) J. Of Alloys and Compounds 183 54-58

[46] Kianvash A. and Harris I. R. (1992) J. Of Alloys and Compounds 178

[47] Ragg, O.M and Harris I.R, (1997) *A study of the effects of the addition of various amounts of Cu to sintered Nd-Fe-B magnets* J. of Alloys and Compounds Vol 256 1-2 p 252-257

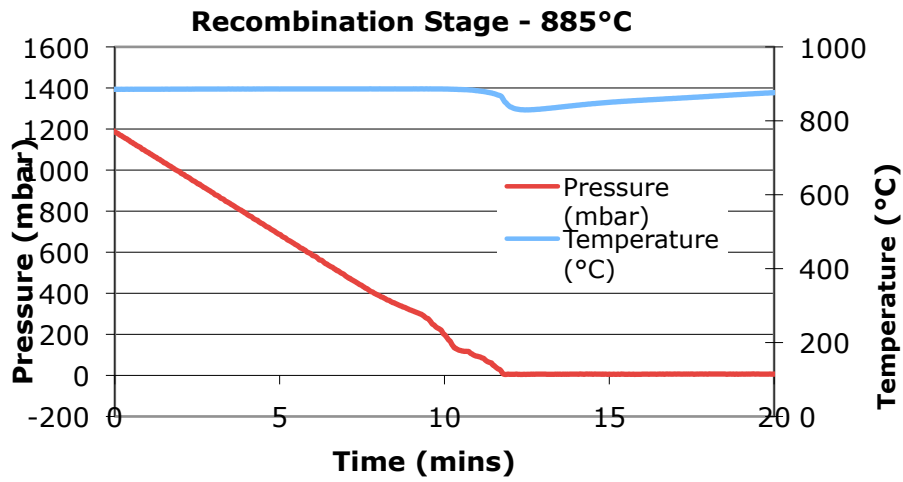
[48] Tokunga M, Harada H. and Trout S. R. (1987) IEEE Transactions of Magnets, 23 No. 5 2284-2286

- [49] Tokunga M, Kogure H, Endoh M. And Harada H. (1987) IEEE Transactions of Magnets 23 No. 5 2287-2289
- [50] Allibert C. H. (1989) Journal of Less Common Metals 152 L1-L4
- [51] Rodewald and Wall (1989) *Structure and magnetic properties of sintered NdFeNbB magnets*. J of Magnetism and Magnetic Materials 80 1 p 57-60
- [52] Corfield M. R, Harris I. R and Williams A. J (2008) *Journal of Alloys and Compounds* 463 180-188
- [53] German R. M, (1996) Sintering Theory and Practice. Wiley. New York 226
- [54] Walton A., Yi H., Rowson N., Speight J.D., Harris I.R. and Williams A.J (2012) *The Use of Hydrogen to Separate and Recycle NdFeB Magnets from Electronic Waste*, Japan REMP conference.
- [55] Zakotnic M, Harris I.R. and Williams A.J. (2009) *Mutliple Recycling of NdFeB-type sintered magnets*. J. of alloys and compounds 469. Pg 314-321
- [56] Rivoirard, Noudem J.G., de Rango P., Fruchart D., Liesert S. and Sobeyroux J.L, (2000) Proceedings of the 16th International Workshop on Rare Earth Magnets and their Applications, Japan, p355.
- [57] Sheridan R.S., Siltoe R., Zakotnic M., Harris I.R. and Williams A.J. (2012) *Anistropic powder from sintered NdFeB magnets by the HDDR processing route* Journal of Magnetism and Magnetic Materials 324 p63-67
- [58] Zhang X.J, Yin X.J, McGuiness P.J and Harris I.R. (1995) *Metallurgical processing of Nd₂Fe₁₄B type permanent magnet alloys*, J. of Materials Processing Technology 48, p461-467
- [59] Siltoe R, (2009) Final Year Project, University of Birmingham.
- [60] Sheridan R.S. (2009-2013) PhD Thesis, University of Birmingham
- [61] Skulj I, Evans H.E. and Harris I.R., (2008) *Oxidation of NdFeB type magnets with modified Co, Dy, Zr and V*, J. of Materials Science, 43 4 1324-1333
- [62] Sun A., Wu S., Xu W., Wang J., Zhang Q., Zhai F. and Volinsky A., (2012) *Nd₂Fe₁₇ nanograins effect on the coercivity of HDDR NdFeB magnets with low boron content*. Int J. Minerals, Metallurgy and Materials 19,3, p236
- [63] Book D. and Harris I.R. (1995) *Hydrogen absorption/desorption and HDDR studies on Nd₁₆Fe₇₆B₈ and Nd₁₃Fe₈₂B₆* Journal of Alloys and Compounds 221 187-192
- [64] Morimoto K., Katayama N, Akimine H and Itakura M. (2012) *Coercivity enhancement of anisotropic Dy-free Nd-Fe-B powders by conventional HDDR process* Journal of Magnetism and Magnetic Materials, Vol324, I 22, p. 3723-3726

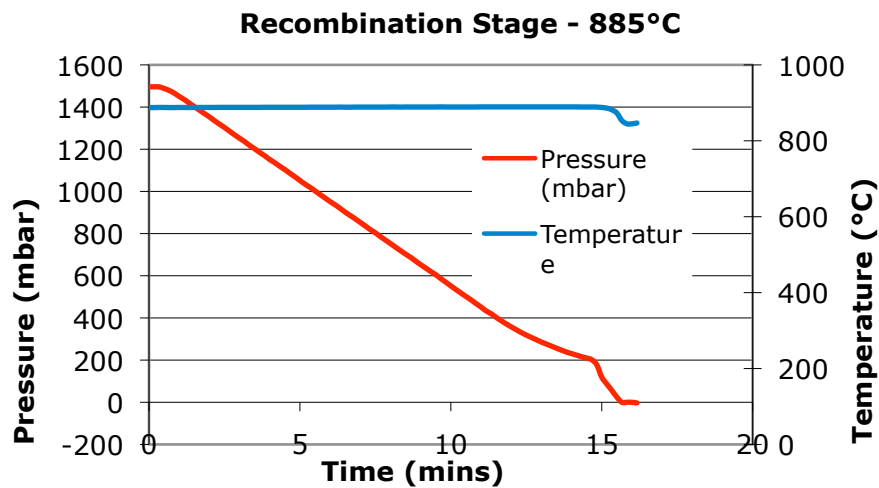
[65] Campbell A. (2013) Final Year Project, University of Birmingham.

Appendix

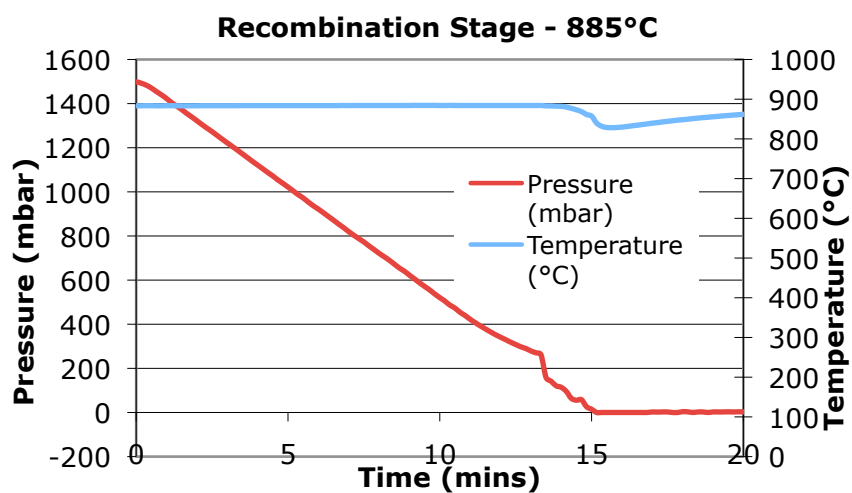
Recombination Curve: Sintered $\text{Nd}_{13}\text{Fe}_{78}\text{Al}_{0.7}\text{Dy}_{0.8}\text{B}_{6.3}$



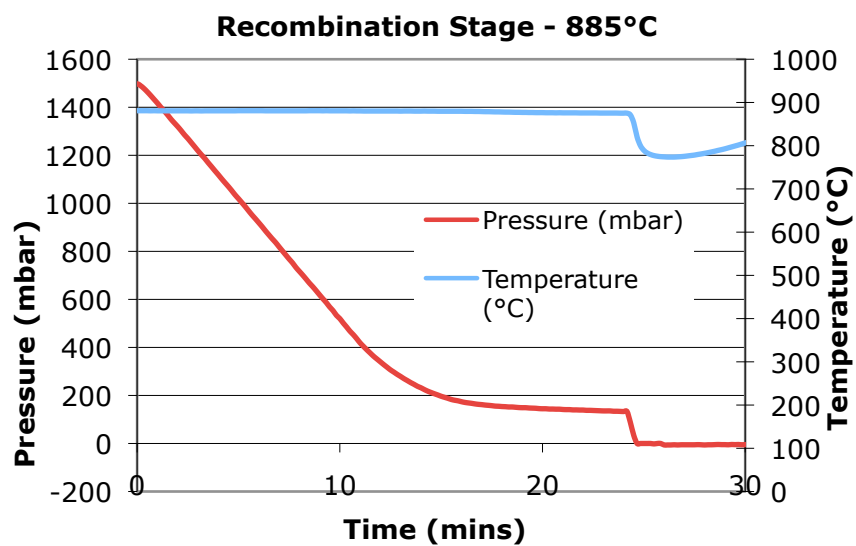
Recombination Curve: Arc melted $\text{Nd}_{13}\text{Fe}_{78}\text{Al}_{0.7}\text{Dy}_{0.8}\text{B}_{6.3}$



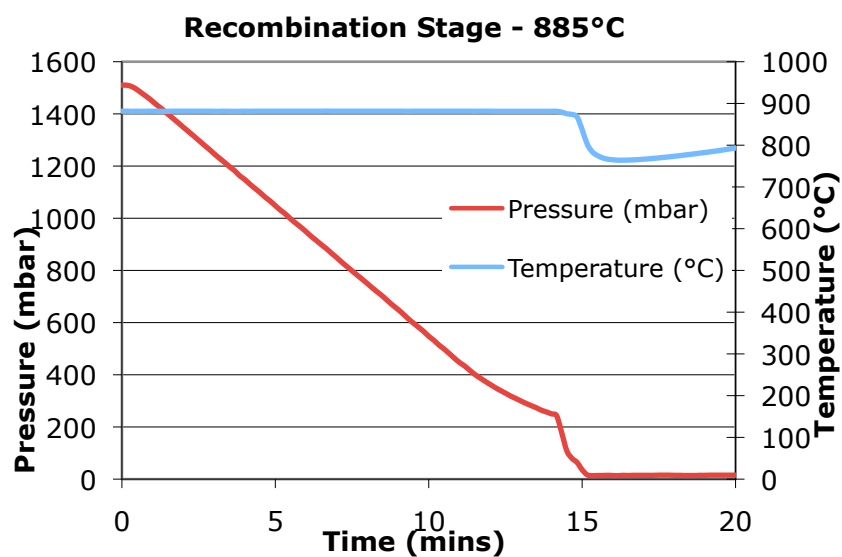
Recombination curve: Annealed $\text{Nd}_{13}\text{Fe}_{78}\text{Al}_{0.7}\text{Dy}_{0.8}\text{B}_{6.3}$



Recombination Curve: Philips Magnet $\text{Nd}_{11.6}\text{Fe}_{77.9}\text{Co}_{1.4}\text{Pr}_{1.6}\text{Dy}_{0.5}\text{B}_6$



Recombination Curve: Cast $\text{Nd}_{13}\text{Fe}_{78}\text{Al}_{0.4}\text{B}_{7.4}$ alloy



Re combination Curve: Cast $\text{Nd}_{15.6}\text{Fe}_{75}\text{Al}_{0.7}\text{B}_{8.2}$ alloy

